2019

The Effects of 3D Printing Parameters and Surface Treatments on Convective Heat Transfer Performance

Lucas N. Pereira
South Dakota State

THE EFFECTS OF 3D PRINTING PARAMETERS AND SURFACE TREATMENTS ON CONVECTIVE HEAT TRANSFER PERFORMANCE

BY

LUCAS N. N. PEREIRA

A thesis submitted in partial fulfillment of the requirements for the

Master of Science

Major in Mechanical Engineering

South Dakota State University

2019

THE EFFECTS OF 3D PRINTING PARAMETERS AND SURFACE TREATMENTS ON CONVECTIVE HEAT TRANSFER PERFORMANCE

LUCAS N. N. PEREIRA

This thesis is approved as a creditable and independent investigation by a candidate for the Master of Science degree and is acceptable for meeting the thesis requirements for this degree. Acceptance of this does not imply that the conclusions reached by the candidate are necessarily the conclusions of the major department.

Todd Letcher, Ph.D.
Thesis Advisor Date

Kurt Bassett, Ph.D.
Head, Department of Mechanical Engineering Date

Dean, Graduate School Date

I dedicate this work to my family, girlfriend and loved ones for their support throughout my studies. Their encouragement and advice helped me to succeed as a person and student.

ACKNOWLEDGEMENTS

I wish to express my sincere appreciation to Dr. Todd Letcher, my thesis advisor, for all that he has done for me throughout my undergraduate, and especially graduate, studies. His knowledge, encouragement, and support were fundamental to my success. I also wish to thank him for his availability.

I would like to thank Dr. Gregory Michna for his guidance and knowledge throughout my studies. His advice about my coursework as well as his knowledge of heat transfer was much appreciated throughout my research.

I also wish to thank Dr. Zhong Hu, graduate coordinator, and the numerous faculty members of South Dakota State University who I had the pleasure to work with and learn from during my undergraduate and graduate studies. The opportunity to work as a Graduate Teaching Assistant was very beneficial for me both in terms of financial assistance during my studies, as well as the knowledge I gained from teaching and engaging with students from a different point of view.

Lastly, I wish to thank my family, my girlfriend and loved ones for their support, love, and patience throughout my studies.

CONTENTS

ABBREVIATIONS

3d	Three Dimensional
A	Surface Area of ABS tube
ABS	Acrylonitrile Butadiene Styrene
AM	Additive Manufacturing
CAD	Computer Aided Design
D	Diameter
FFF	Fused Filament Fabrication
HTC	Heat Transfer Coefficient
h_c	Heat transfer Coefficient
I	Current
k	Thermal conductivity of the working fluid
LH	Layer Height
Nu	Nusselt Number
P	Power
PETG	Polyethylene Terephthalate Glycol-Modified
PHX	Polymer Heat Exchanger
PLA	Polylactic Acid
Pr	Prandtl Number
Re	Reynolds Number
q''	Heat flux
SLA	Stereolithography
SLS	Selective Laser Sintering
STL	Standard Tessellation Language
$T_{o,ABS}$	Surface temperature at ABS tube
T_∞	Inlet temperature inside wind tunnel
V	Voltage
v	Velocity of the fluid
ν	Kinematic viscosity of air

LIST OF FIGURES

LIST OF TABLES

ABSTRACT

THE EFFECTS OF 3D PRINTING PARAMETERS AND SURFACE TREATMENTS ON CONVECTIVE HEAT TRANSFER PERFORMANCE

LUCAS N. N. PEREIRA

2019

Additive manufacturing technology and applications have quickly expanded in many industries over the last five years. As additive manufacturing is studied and refined, improvements in resolution and strength have helped propel further growth of the industry. This study focuses on an additive manufacturing technology called fused filament fabrication (FFF). FFF involves the extrusion and layer-by-layer deposition of a molten thermoplastic material to create the desired part. One potential new application of fused filament fabrication is the manufacture of heat exchangers and heat sinks. This study focuses on developing baseline experimental data related to convective heat transfer coefficients over surfaces of commonly used polymers in FFF 3d printing while varying printing parameters and surface treatments of the samples.

A copper pipe containing two cartridge heaters was placed inside the ABS test samples with two thermocouples placed at the surface of the 3d printed material to measure the surface temperature of the cylinder. The samples were tested inside a wind tunnel to measure the effects of surface roughness and printing parameters on heat transfer over a range of velocities.

Samples with different printing parameters were tested first. Parts with layer heights (LH) of 0.1 mm, 0.2 mm and 0.3 mm were printed. As the layer height increases the roughness also increased. Sample 1 of LH = 0.1 mm had a roughness of 9.72 µm and a heat transfer coefficient of 72 W/m^2-K and sample 1 of LH = 0.3 mm had a roughness of 28.83 µm and a heat transfer coefficient of 85 W/m^2-K, with fans operating at 12V. Surface treatment, such as acetone smoothing, sanding and sanding/acetone-smoothing were performed in other to reduce surface roughness. The acetone smoothing process affected more the samples with smaller layer heights. Sample 1 of LH = 0.2 mm had a roughness reduced to 11.43 µm and a heat transfer coefficient of 71 W/m^2-K. Sanding and sanding/acetone-smoothing process recorded the smallest values for roughness, while recording the highest values for heat transfer coefficient. Sanded sample 2 of LH = 0.3 had a heat transfer coefficient of 101 W/m^2-K and roughness of 4.35 µm.

INTRODUCTION

Additive manufacturing (AM), also known as 3d printing, is a manufacturing process designed to build 3d objects by adding material layer by layer. AM technology and applications have been developing quickly over the last five years. As AM is studied and refined, aspects of manufacturing, such as resolution and strength, have helped propel further growth of the industry [1]. The process consists of designing a 3d model in a computer-aided design (CAD) software and transferring the file to the printer via an SD card. Some Additive Manufacturing techniques are selected laser sintering (SLS), fused filament fabrication (FFF), stereolithography (SLA), and digital light processing (DLP). This study will focus on FFF, in which a molten thermoplastic material is extruded and deposited layer by layer to create the desired part. Some examples of the thermoplastic materials are the polylactic acid (PLA), polyethylene terephthalate glycol-modified (PETG), polyamide (Nylon), and acrylonitrile butadiene styrene (ABS) [1, 2].

Recently, an area of study that has been receiving a lot attention is the use of 3d printed parts for heat transfer applications, such as heat exchangers and heat sinks. A heat exchanger is a device designed to transfer heat between two or more fluids. It is commonly used in space heating and air conditioning. A heat sink is a passive heat exchanger that transfers the heat generated by an electronic or mechanical device to a fluid medium, usually air or liquid coolant. A common use of heat sinks is in the central processing units (CPU) of computers. The design, choice of material, air velocity, and surface treatment are factors that can affect the performance of heat exchangers and heat sinks.

Recently, polymers have been studied as an alternative option to traditionally used materials, such as copper and aluminum. Some of the benefits of using polymers are that

polymers are light-weight, easily manufactured, inexpensive, and non-corrosive [2]. However, polymers have low thermal conductivity and since this is a recent area of study, there is very literature to review. Therefore, the heat transfer performance of these polymers at different surface conditions is still very unclear. So the heat transfer properties of polymers and its relation to the surface roughness in different circumstances could possibly help the development of polymer heat exchangers with similar or better performance to the metal heat exchangers. Hence, this study will focus on developing baseline experimental data related to convective heat transfer coefficients over surfaces of commonly used polymers in FFF 3d printing while varying printing parameters and surface treatments of the samples.

LITERATURE REVIEW

Several researchers have analyzed the performance of 3d printed parts on heat transfer applications. Over the past couple of years the focus has been on the innovation, characterization and implementation of polymer heat exchanger (PHX) technology due to some benefits that comes within the material such as low cost, no corrosion and easy to manufacture. Also, new polymers with higher temperature limits, higher impact and yield strength and higher thermal conductivities could possibly help these polymer heat exchangers have a similar or better performance to the metal heat exchangers.

Arie et al. [3] fabricated and tested a polyethylene heat exchanger. The flow channels were 15.5 cm wide and 29 cm long. For the water-to-air heat exchanger had an air-side flow rate of 3-24 L/s and water-side flow rate of 12.5 mL/s, and the overall heat transfer coefficient was in between 35-120 W/m^2-K. The air-side performance of the PHX was compared with the performance of two commercially available metallic plain plate fin heat exchanger surfaces. The plate performance was calculated and then compared. PHX had an equal or even superior performance for the same pressure drop, which shows some promise in competing with conventional heat exchangers. In addition, it was found that the wall thermal resistance is not a limiting factor for low thickness, because it only represented up to 3% of the total thermal resistance.

Michna et al. [4] tested ABS heat exchangers with different designs. The objective was to maximize the heat transfer from water, which enters the heat exchanger at 60ºC, to the room temperature air blown over the outside. The dimension of the heat exchangers were 100 × 100 × 20 mm and the best design provided a heat transfer rate of 61.2 W. Due

to the low conductivity of the ABS plastic, the heat exchangers had a variety of geometries in order to maximize the heat transfer.

In another study, Felber et al. [5] designed and tested an ABS heat exchanger. The prototype was designed with nine air channels and five two-pass water channels and its performance was compared to that expected from the model. At higher velocities, the experimental and predicted thermal data were similar. At an air velocity of 1.25 m/s, analytical and experimental data recorded a heat transfer rate around 60 W. However at lower velocities, the experimental data deviate. At an air velocity of 0.35 m/s, analytical data calculated a heat transfer rate around 38 W, while experimental data recorded heat transfer rate around 25 W. At the end of the study, it was found that the heat transfer performance could be improved by improving the thermal conductivity. Increasing the thermal conductivity from 0.2 to 2 W/m-K has a greater effect than increasing from 2 to 20 W/m-K.

Wu et al. [6] measured the heat transfer characteristics for the flow of gas in the fine channels of heat exchangers used for micro miniature refrigerators. The unique feature about the channels in this heat exchanger is their asymmetric roughness, large relative roughness and large variation of heat flux and temperature of the walls. The roughness of the channels can have an impact in the heat transfer coefficient. In this study, the shape and size of the roughness was undefined and random due to an etching process occurred earlier in the experiment. The rougher channels had an improved heat transfer coefficient but also an increase in the friction factor when compared to the smother channels.

Surface roughness is a factor that has a significant influence on performance in convection heat transfer applications [7]. Some studies concerning the effects of surface roughness on heat transfer are available. Achenbach et al. [8, 9] performed a study of the influence of the surface roughness on the cross flow around a circular cylinder. Reynolds number, local pressure and skin friction distribution were measured and the total drag, pressure drag and friction drag were calculated. By means of the skin friction, the position of separation point can be localized and the flow can be defined into three states. Higher roughness caused strong disturbances and led to premature transition. Also, increasing roughness decreased the critical Reynolds number.

In another study, the influence of surface roughness on heat transfer in transitional flow was studied. The experimental setup consisted of a closed loop which circulated water from a storage tank through the test section and back. The Reynolds, Nusselt, and Prandtl numbers were determined and their relation to the roughness were analyzed. The transition between laminar and turbulent flow occurred earlier with the increase in surface roughness. Heat transfer also increased with surface roughness [10].

Zhang et al. [11] studied the effect of surface roughness on laminar flow and heat transfer characteristics. Microchannels with surfaces with triangular, rectangular and semicircular roughness elements were studied. The geometry of the roughness had a considerable role and as the roughness increased, the flow over triangular and semicircular roughness elements induced stronger recirculation and flow separation, which improved heat transfer performance but also increased the pressure drop.

Wu et al. [12] performed an experimental study on the laminar convective heat transfer and pressure drop in silicon microchannels with different surface conditions. The laminar Nusselt number and apparent friction constant increase with the increase of surface roughness. This change was more visible at larger Reynolds number. Also, this increase happened faster at high roughnesses since the disturbance in the boundary sub layer is more significant at high Reynolds number. Microchannel #7 had a roughness of $3.26\times10^{-5}$and microchannel #9 had a roughness of 5.87×10^{-3}. At a Reynolds number of 800, the Nusselt number for microchannel #7 was around 2.7, while at #9 the Nusselt number increased to 3.5.

Dierich et al. [13] studied the influence of the roughness on the surface average Nusselt number and drag coefficient past a cylindrical particle over the range of Reynolds number $10 \leq Re \leq 200$. The impact of the roughness on the drag is negligible when compared with the surface averaged Nusselt number. The roughness has a significant impact on the surface average Nusselt number. The Nusselt number decreases rapidly as the degree of roughness of surface roughness increases.

Kandlikar et al. [14] completed a study on the effect of surface roughness on heat transfer at low Reynolds numbers in a small diameter tube. The tube was tested with its original surface and with two acid treatments. Heat transfer properties were measured and calculated in order to compare the different samples. The first acid treatment reduced the roughness (from 2.4 to 1.9 microns) and therefore, reducing the heat transfer coefficient and pressure drop values. However, after the second acid treatment, the roughness increased (from 2.4 to 3 microns).

Even though some experimental and theoretical studies focusing on finding the effects of surface roughness on heat transfer have been performed recently, this area can still be widely studied because of the variety of experimental apparatuses, processing parameters, material properties, and surface roughness.

METHODS

Different from the previous studies, which tested the effects of roughness of mostly metal parts, the test sample for this experiment is a 3d printed ABS tube with an outside diameter of 9.8 mm and inside diameter of 8.2 mm. A convective heat transfer analysis in a circular polymer tube was used to find the heat transfer coefficient of 3d printed components. Cylinders with different printing parameters and surface roughness were tested and compared. The first set of samples consisted of ABS cylinders 3d printed with several layer heights. Layer height is the thickness of each layer of the 3d printed part. Parts printed with a larger layer height are not as visually appealing. However, printing at larger layer heights is faster, and therefore, less expensive, and in some cases, shows improved mechanical strength. Thinner layer heights are usually used for parts that require better visual appearance. Thinner layers require more time and cost, due to more machine time [15]. For this work, samples with layer heights of 0.1 mm, 0.2 mm, and 0.3 mm were printed. With the purpose of having a variety of surface roughness, some samples had common 3d printed surface finishing techniques applied, including an acetone smoothing process, sanding, and both sanding and acetone smoothing on the same sample. Acetone smoothing process consisted of acetone being applied to paper towel, which was then applied to the surface of the ABS sample. The acetone was applied from one end to the other end of the cylinder. The sanding treatment consisted of the ABS cylinder being in contact with a belt sander. The sanding/acetone treatment consisted of the sanding process occurring first and the acetone smoothing occurring after. Figure 1 illustrated in each direction each treatment was being applied on. Figure 2 show a sample of each layer height. As the layer height increases, it becomes easier to see each layer of the part. Figure 3 show sample with LH = 0.3 before and after surface treatment.

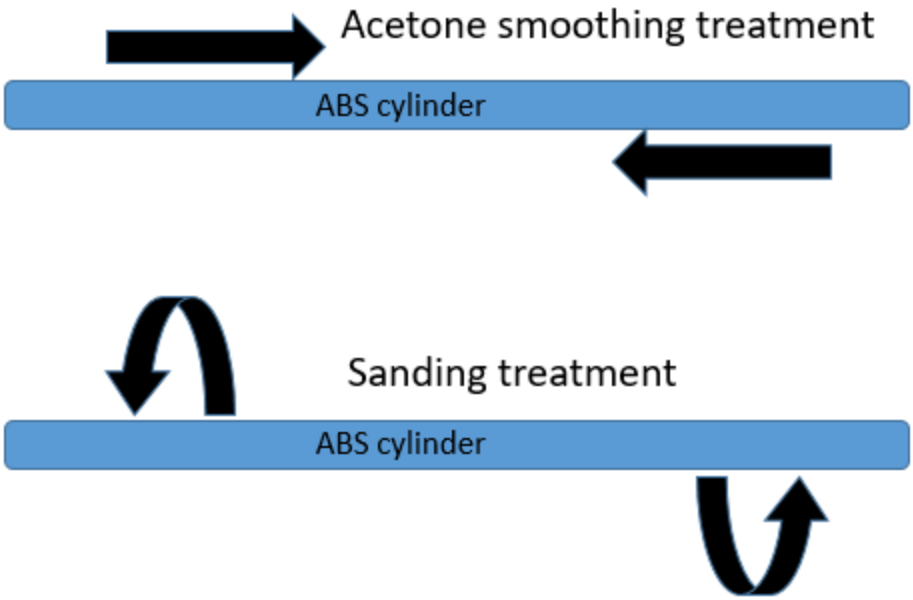

Figure 1. Direction of the acetone smoothing and sanding treatments.

Figure 2. Examples of 3d printed ABS tubes test before surface treatment - Layer height = 0.1 mm (left), Layer Height = 0.2 mm (center), Layer Height = 0.3 mm (right).

Figure 3. 3d Printed ABS tube with 0.3mm layer height and surface treatments applied – (From left to right) No surface treatment, rubbed acetone treatment, sanding, and sanding followed by rubbed acetone treatment.

A copper pipe, with an outside diameter of 8.1 mm and inside diameter of 6.3 mm, containing two cartridge heaters (6.3 mm diameter) inside it, was placed inside the ABS test sample with two thermocouples placed at the surface of the 3d printed material to measure the surface temperature of the cylinder. A copper pipe was chosen because copper has one of the highest thermal conductivities, giving superior heat spreading ability. Therefore, the copper pipe was ideal to conduct heat from the cartridge heaters to the ABS tube, distributing heat throughout the ABS tube as uniformly as possible. Both cylinders had a length of 112 mm, and the total length exposed to the air flow was 100 mm. In order to improve the thermal connections, a thermal paste was used on the surface of the cartridges heaters, copper pipe and at the thermocouple location. The thermal paste used was a silicone heat transfer compound, catalog number 860-150G from MG Chemical. It

has a thermal conductivity of 0.66 W/m-K. Figure 4 shows the heater cartridges, copper tube and ABS sample assembled and schematics showing the cross section of the sample.

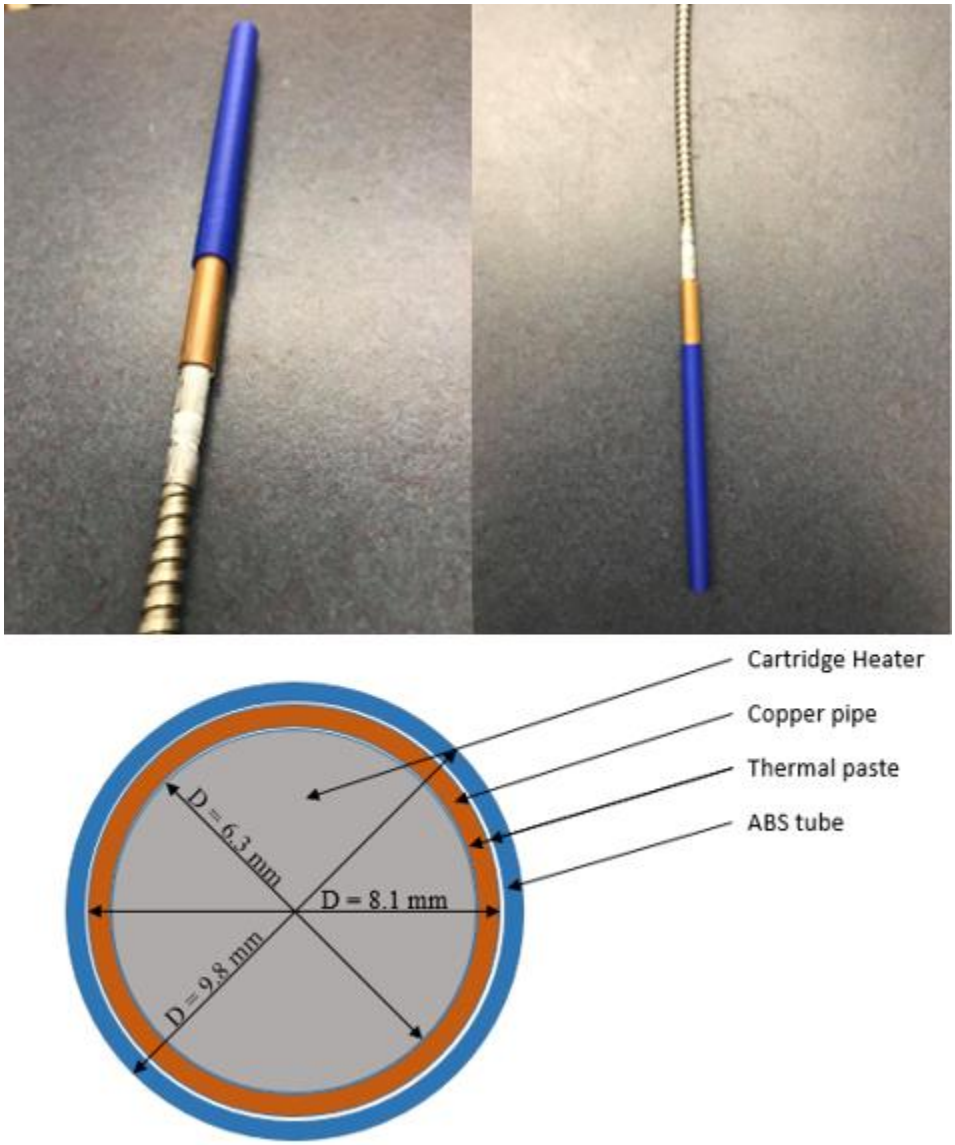

Figure 4. Top: ABS tube, copper pipe and cartridge heaters. Bottom: Cross-section of test sample.

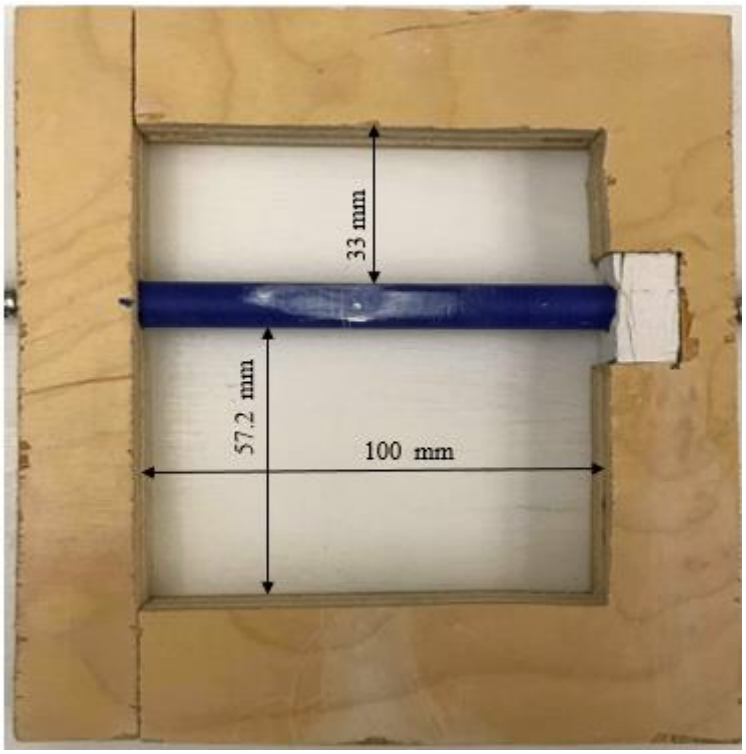

Figure 5. Test sample and thermocouple location inside wind tunnel mounting plate.

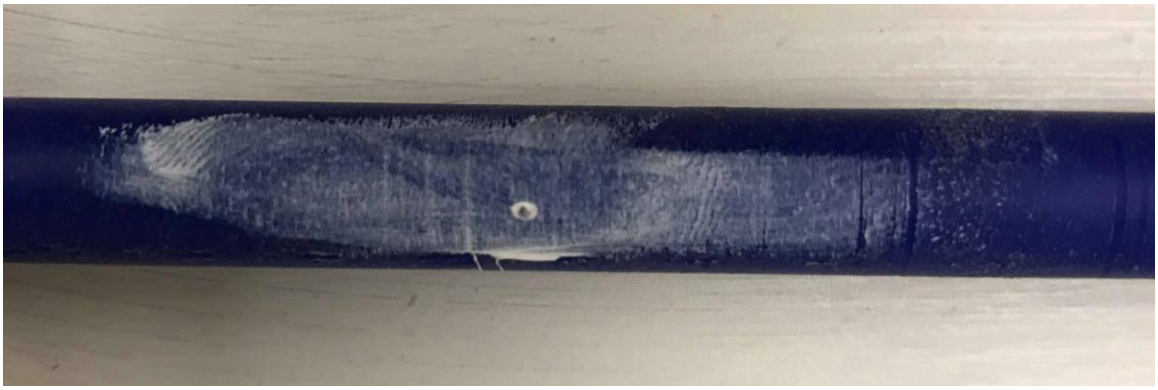

Figure 6. Close up view of the test sample with thermocouple hole.

The samples were tested inside a wind tunnel. The test sample was placed in a wood test section (Figure 5), and the test section was installed in the wind tunnel. Four 12V DC fans (model PFM0812HE-01, Delta Electronics, Inc.), were used in the wind tunnel, and their speed was regulated by a power supply. The voltage of the fans varied from 5 V to 12

V, which created different air velocities ranging from about 10 m/s to 23 m/s. The power applied and air velocity for all voltages are shown in Table 1. The velocity of air varies at different heights inside a wind tunnel. The highest velocity is reached in the middle of the tunnel, and as the flow gets closer to the bottom and top, the velocity decreases to near zero due to the presence of the boundary layer. Figure 7 shows the velocity profile inside the wind tunnel with fans at 12 V along the transverse centerline. The sample is located at a height of 60 mm, with the thermocouple located along the transverse centerline and the velocity measurements during the study were recorded at that height.

Table 1. Power and velocity values calculated for different fan voltage.

Fan Voltage (V)	Power (W)	Flow Velocity (m/s)
12	9.96	22.65
11	9.65	21.33
10	9.44	18.75
9	9.18	17.62
8	8.98	16.15
7	8.75	13.95
6	8.57	12.03
5	8.27	10.37

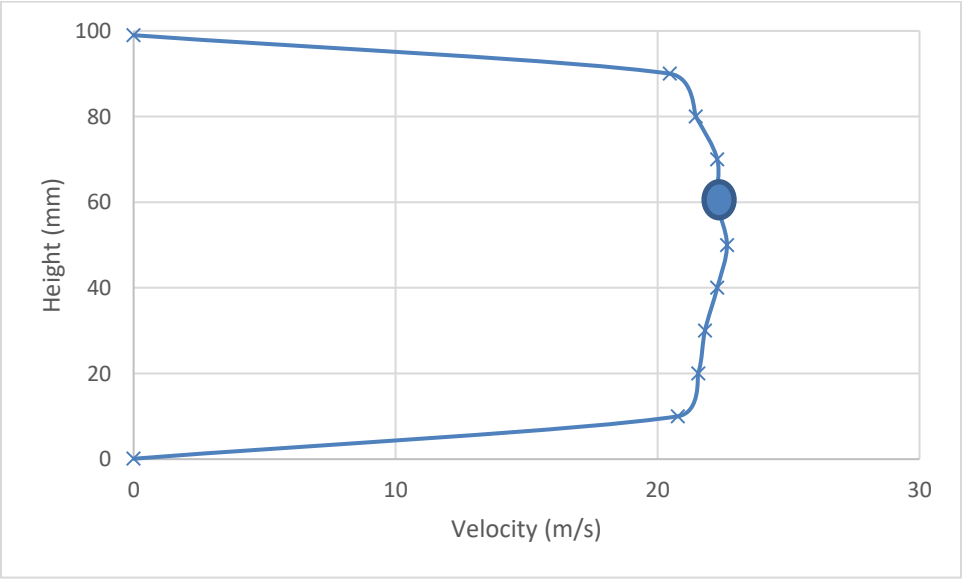

Figure 7. Velocity profile at different heights inside the wind tunnel at 12V.

Type T thermocouples were used to measure the temperatures during the test. Three thermocouples recorded the air temperature at the inlet and the outlet of the wind tunnel, and another thermocouple recorded room temperature outside the wind tunnel. Two thermocouples were used to measure the surface temperature of the ABS tube. These thermocouples were placed through two holes, 180 degrees apart in the middle of the ABS tube, which was located during testing along the transverse centerline of the wind tunnel. To make room for the thermocouple wire, two channels 0.76 mm deep were cut into the copper pipe. The thermocouples were inserted as close as possible to the surface and thermal paste was added to fill the gap around it so the measured temperature was as close as possible to the surface temperature. The thermocouples were connected to a data acquisition device (National Instrument thermocouple input module, NI-9213), and LabVIEW software recorded the temperatures values. Figure 8 is a schematic of the experimental apparatus and Figure 8 shows several pictures of the actual wind tunnel setup.

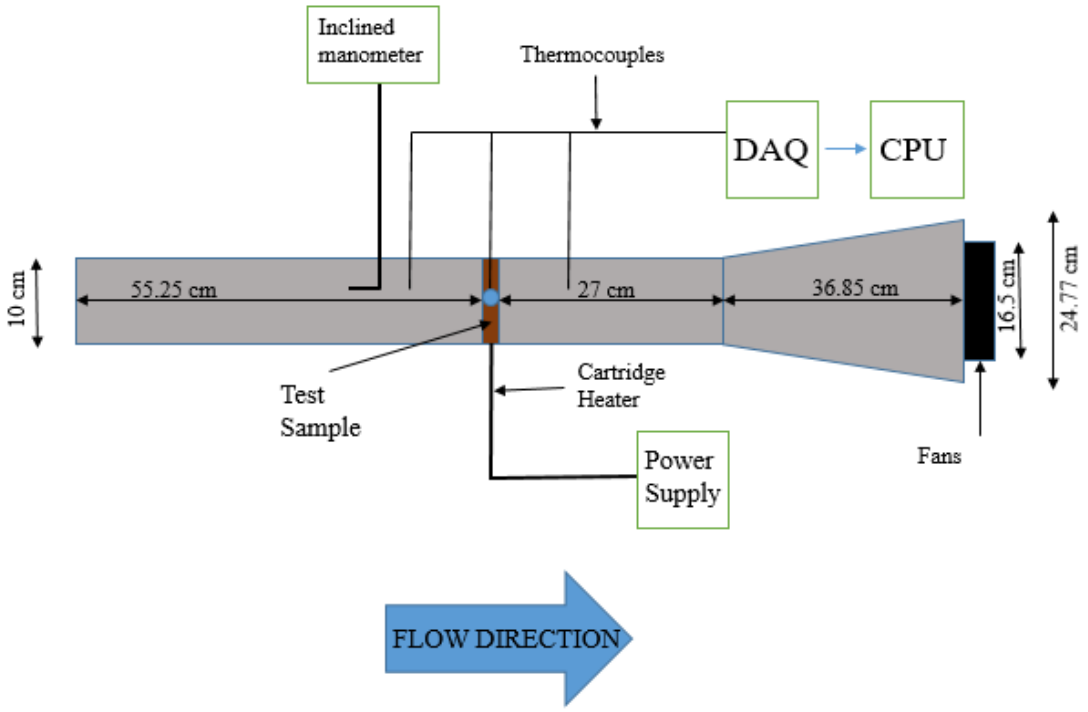

Figure 8. Schematics of experimental apparatus.

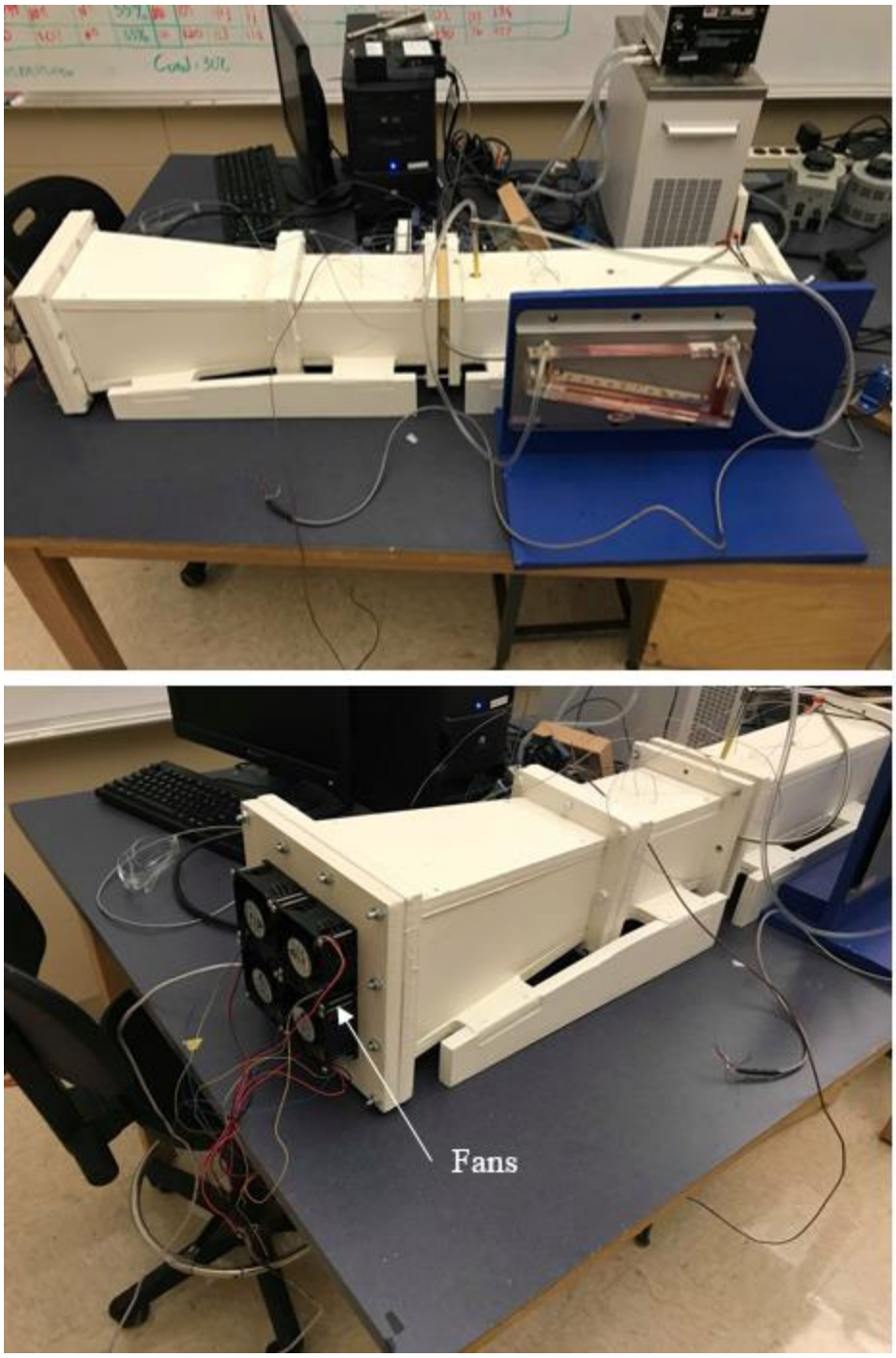

Figure 9. Pictures of experimental apparatus.

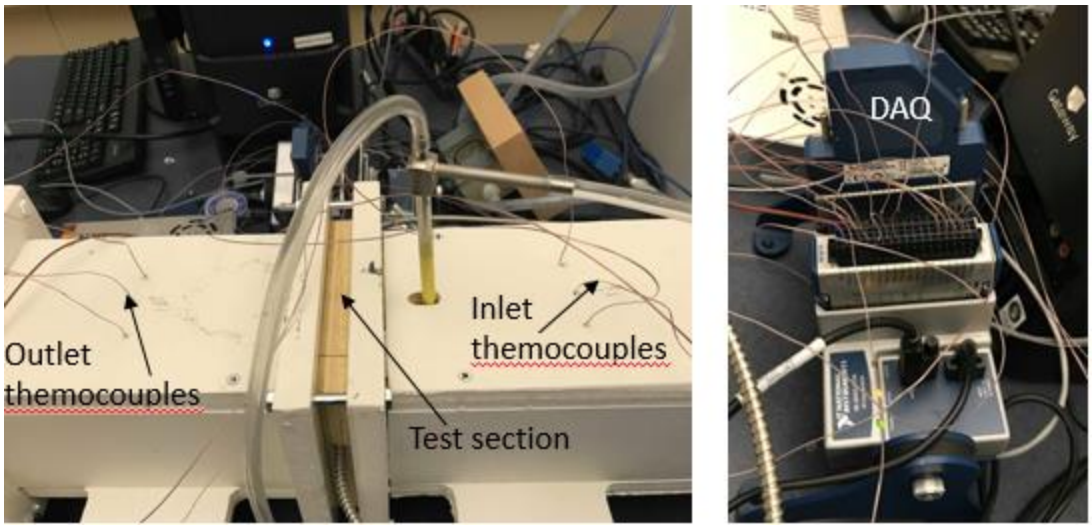

Figure 10. Closer look at test section attached to wind tunnel and thermocouples attached to the DAQ.

Each experiment began by carefully placing the cylinder in the test section in the wind tunnel in the correct orientation. After the cylinder was fixed, the wind tunnel and cartridge heaters were turned on. Initially, the fan voltage was set to 12 V to obtain maximum air speed. The velocity of the air inside the tunnel was determined with a pitot-static tube placed inside and after the measurements, the pitot-tube was removed. The system was allowed to reach equilibrium, and temperature data was recorded for two minutes to obtain average results. After that, the fan voltage was reduced to 11 V and the power to the heater cartridge was adjusted to maintain the same surface temperature of 60°C. After reaching steady state, temperature data was recorded. This process was repeated, reducing the fan voltage by 1 V at a time until reaching 5 V. Then, the sample was rotated 45 degrees and the whole process was repeated again three more time, so at the end of testing, each sample would have an average of eight temperature measurements. Figure 11 shows the LabVIEW Virtual Instrument (VI) used to record the experimental data. Figure 12 shows the location where the temperatures were recorded. In the first run, the temperature was recorded on locations 1 and 5. In the second run, the temperature was

recorded on locations 2 and 6. In the third run, the temperature was recorded on locations 3 and 7. In the fourth run, the temperature was recorded on locations 4 and 8.

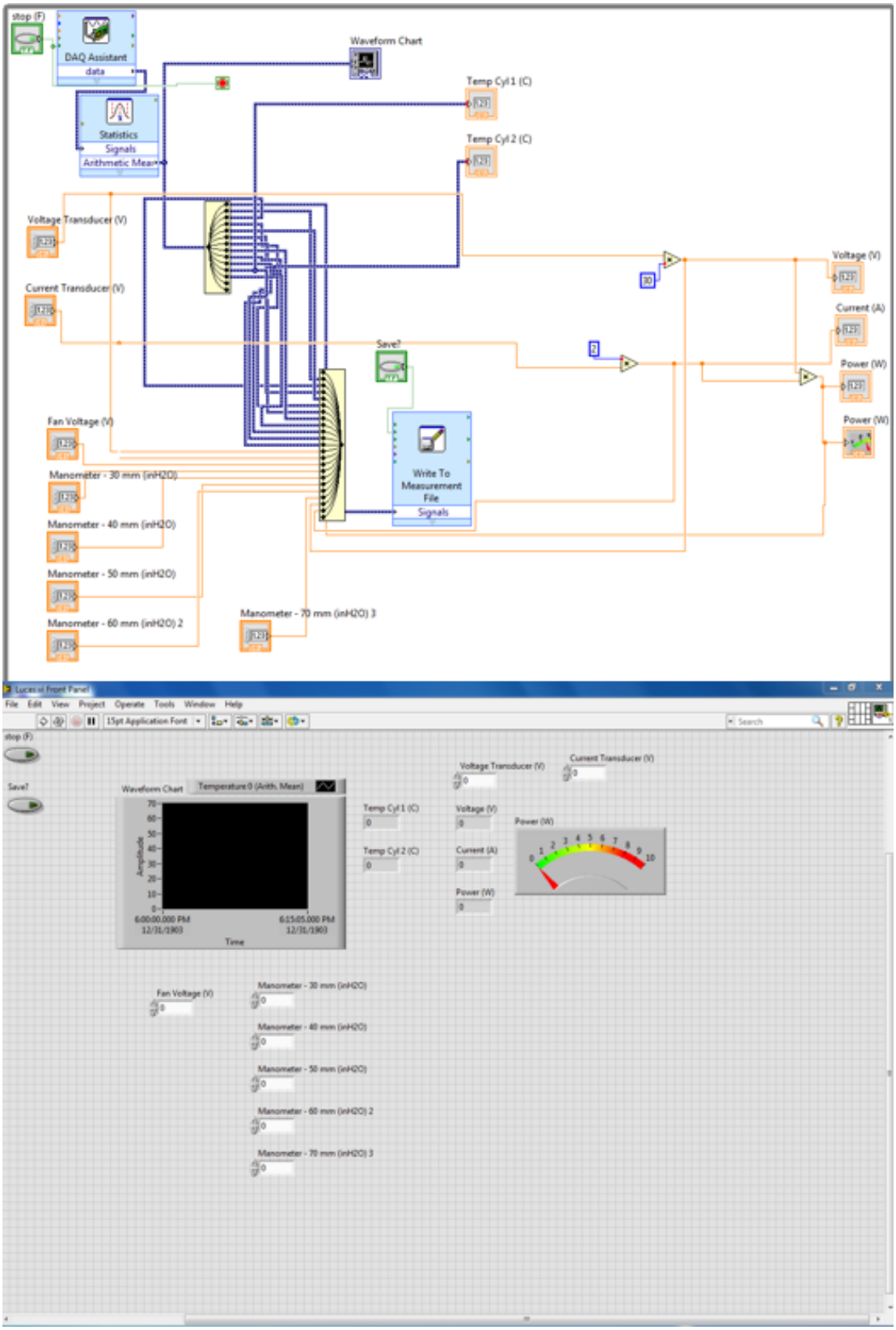

Figure 11. LabVIEW VI.

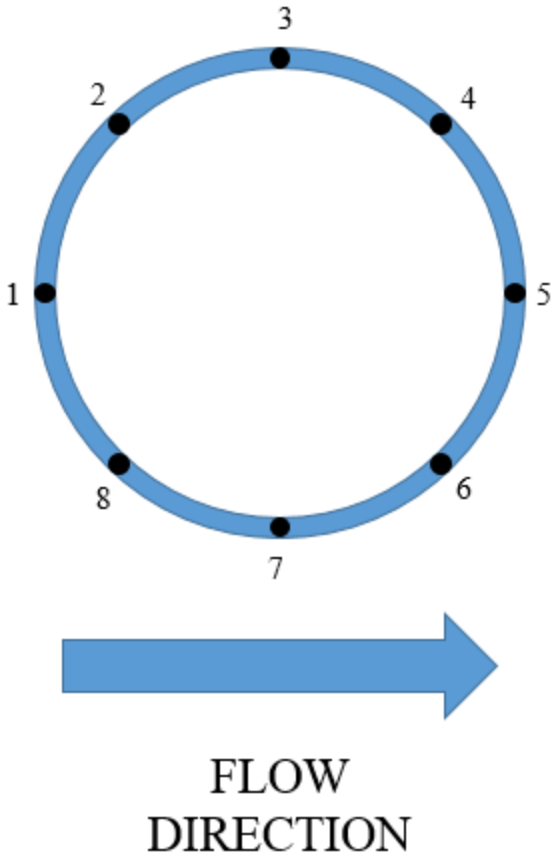

Figure 12. Thermocouple locations where temperature was measured.

The heat transfer coefficient value was calculated using Newton's Law of Cooling, which states that the rate of heat loss of a body is directly proportional to the difference in the temperature between the body and its surroundings provided the temperature difference is small and the nature of the radiating surface remains the same (see Equation 1 [16]).

$$q'' = h_c(T_{o,ABS} - T_\infty) \quad (1)$$

$$P = V \cdot I \quad (2)$$

Convective heat transfer analysis is performed in this scenario and it consists of the transfer of heat between the surface of the ABS cylinder and the air inside the wind tunnel. The heat flux is represented by q'' and represents the flow of energy per unit of area per unit of time. The heat flux was assumed to be uniform for the calculations. During the experiment, the value measured by the power applied to the cartridge heater. Equation 2 was used to find to power applied to the cartridges heater, where P is the total power, V is the voltage and I is current. $T_{o,ABS}$ is the temperature recorded at the surface of the ABS tube and T_∞ is the temperature recorded at the inlet of the wind tunnel.

The Nusselt number was also calculated using Equation 3 [16].

$$\mathrm{Nu} = \frac{\mathrm{h_c \cdot D}}{\mathrm{k}} \tag{3}$$

Nu is the Nusselt number, h is the heat transfer coefficient, D is the diameter of the ABS cylinder and k is the thermal conductivity of the working fluid. The Nusselt number is a dimensionless parameter and provides a measure of the convective heat transfer occurring at the surface. Correlations may be obtained for the Nusselt number. The correlation appropriate to this study was proposed by Churchill and Bernstein. It is an equation that covers the entire range of Reynolds number as well as a wide range of Prandtl number (Pr) and can be used for any cylindrical geometry. The equation is also recommended for all $\mathrm{Re_D \cdot Pr} \geq 0.2$ and can be seen below.

$$\mathrm{Nu_D} = 0.3 + \frac{0.62\mathrm{Re_D^{1/2}Pr^{1/3}}}{[1+\left(\frac{0.4}{\mathrm{Pr}}\right)^{\frac{2}{3}}]^{1/4}}[1 + \left(\frac{\mathrm{Re_D}}{282{,}000}\right)^{\frac{5}{8}}]^{4/5} \tag{4}$$

The Nusselt numbers measured in this study varied from 17, around the small Reynolds number, up to 37 around the larger Reynolds number. The Churchill and Bernstein correlation predicts Nusselt numbers between 40 and 60 for the Reynolds numbers investigated in this research. Due to the wide range of flow conditions, the accuracy of this equation should not be much greater than 20%. The theoretically calculated Nusselt number was quite different from the experimental results. The percentage error was around 50% and it was similar among all samples. The high percentage of error could be the result of the low percentage accuracy of the correlation.

In order to show reliability of the results, the uncertainty was calculated for all measured values. The surface temperature recorded at 12 V was 60°C ± 0.28°C and the ambient temperature was 21.3°C ± 0.28°C. The power applied by the cartridge heaters was 9.85 W ± 0.29 W. The Reynolds number calculated at that voltage was 13,169 ± 232.7. The heat transfer coefficient and Nusselt number were calculated to be 78.4 W/m^2-K ± 0.98 W/m^2-K and 28.7 ± 0.46 respectively. Equation 5 [17] was used to calculated the uncertainty.

$$\omega_R = \sqrt{(\frac{\partial R}{\partial v_1}\omega_1)^2 + (\frac{\partial R}{\partial v_2}\omega_2)^2 + \cdots (\frac{\partial R}{\partial v_n}\omega_n)^2} \quad (5)$$

The surface roughness of each sample was measured using a Keyence 3D laser scanning microscope (20x magnifications) and VK Analyzer software. Figure 13 show how the roughness value was obtained using the Keyence measurement analysis software. It also illustrates the character of roughness of the surface. More detailed microscope scans are shown in Figures 15, 16, and 17. For this paper, surface roughness is reported in "Ra" (arithmetic mean roughness in μm). Ra determines the absolute value of the height

difference between the reference surface and the measured surface. Figure 14 and equation (6) illustrated how the Ra is calculated.

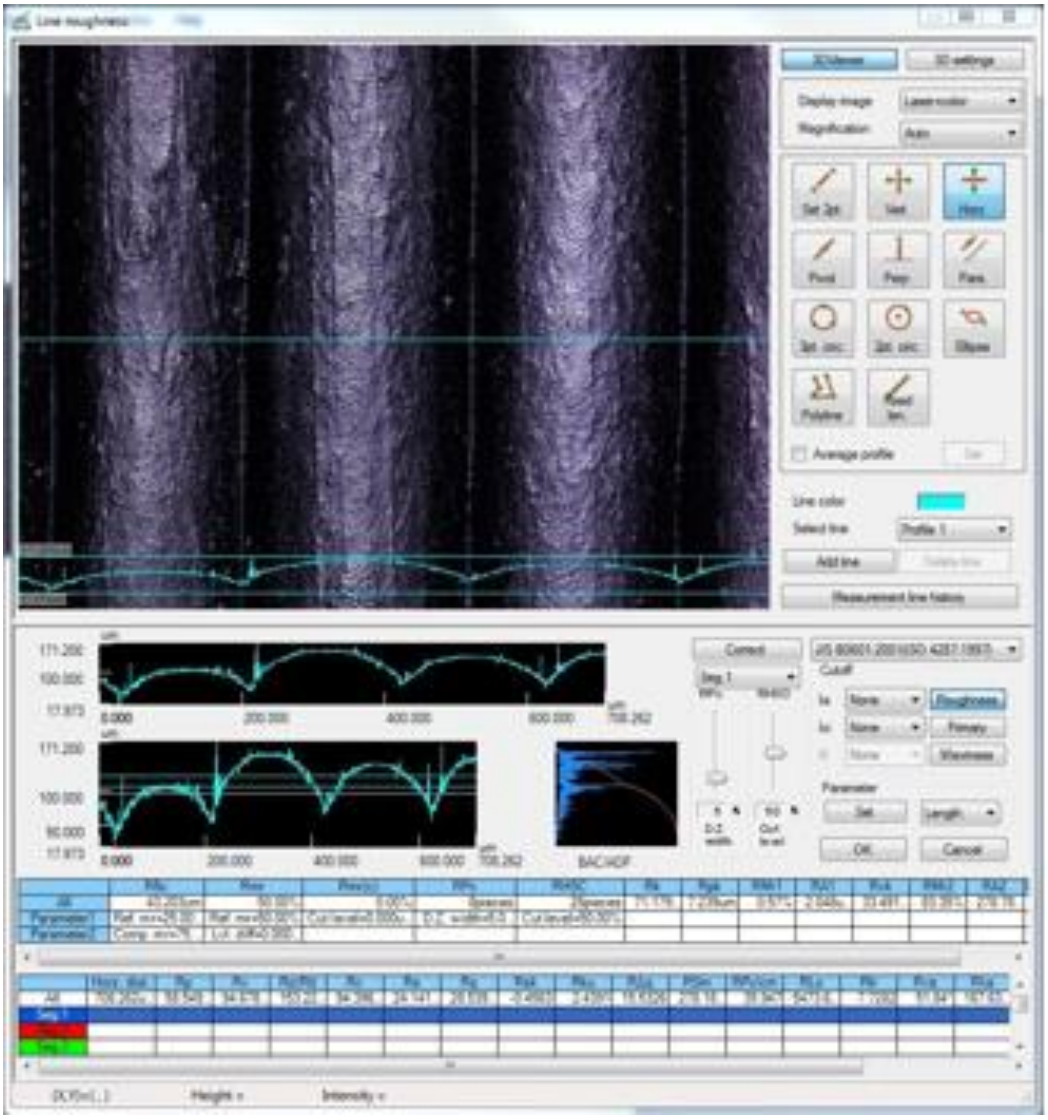

Figure 13. VK Analyzer software used to find line roughness values.

$$Ra = \frac{1}{l}\int_0^l |f(x)|dx \qquad (6)$$

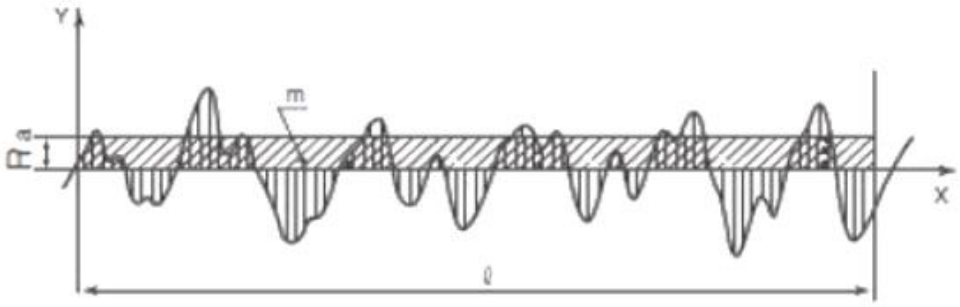

Figure 14. Illustration of how the RA is obtained.

RESULTS

Before testing, surface roughness values were measured for each of the samples. The values found for roughness in each sample are shown on Tables 2, 3 and 4. Before any surface treatments, the samples with the highest surface roughness were the samples with LH = 0.3 mm, with roughness values of about 29 μm, and the samples with the lowest surface roughness were samples with LH = 0.1 mm, with roughness values of about 10 μm. After surface treatment, the roughness values varied differently for each treatment. Samples that were acetone smoothed had roughness values reduced by a small amount. Samples that were sanded showed a significant change to the surface roughness with values between 3 and 5 μm. Samples that were sanded and acetone smoothed had a roughness between 0.8 and 2 μm.

Table 2. Surface roughness (μm) on samples with LH = 0.1 mm.

No Surface Treatments						
LH = 0.1mm	**Sample 1**	**Sample 2**	**Sample 3**			
Roughness (Ra)	9.72	13.76	10.06			
After Surface Treatment						
	Acetone 1	**Acetone 2**	**Sanding 1**	**Sanding 2**	**Sanding-Acetone 1**	**Sanding-Acetone 2**
Roughness (Ra)	9.8	10.95	4.99	3.39	1.17	0.85

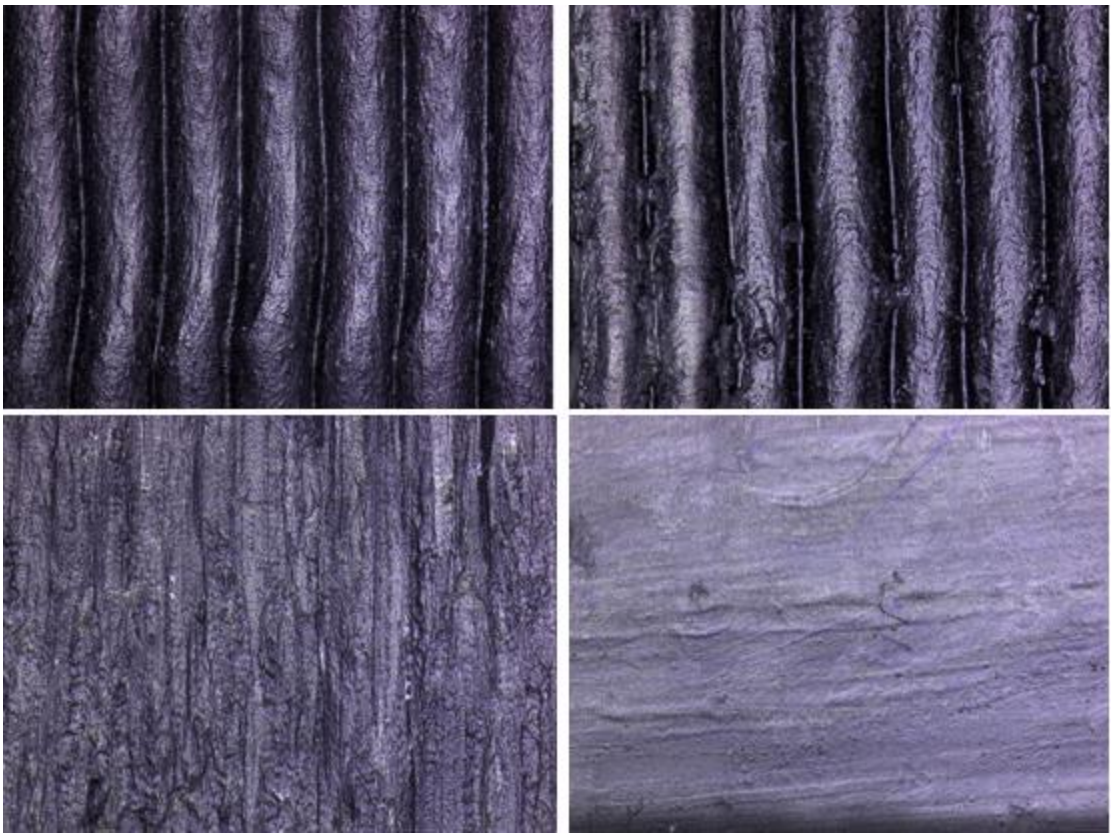

Figure 15. Microscopic pictures of LH = 0.1 mm samples. Top-left: untreated; Top-right: acetone-smoothed; Bottom-left: sanded; Bottom-right: sanded/acetone-smoothed. Lens 20X.

Table 3. Surface roughness on samples with LH = 0.2 mm.

No Surface Treatments						
LH = 0.2mm	**Sample 1**	**Sample 2**	**Sample 3**			
Roughness (Ra)	24.66	21.06	17.36			
After Surface Treatment						
	Acetone 1	**Acetone 2**	**Sanding 1**	**Sanding 2**	**Sanding-Acetone 1**	**Sanding-Acetone 2**
Roughness (Ra)	11.43	14.24	3.26	3.33	1.32	1.19

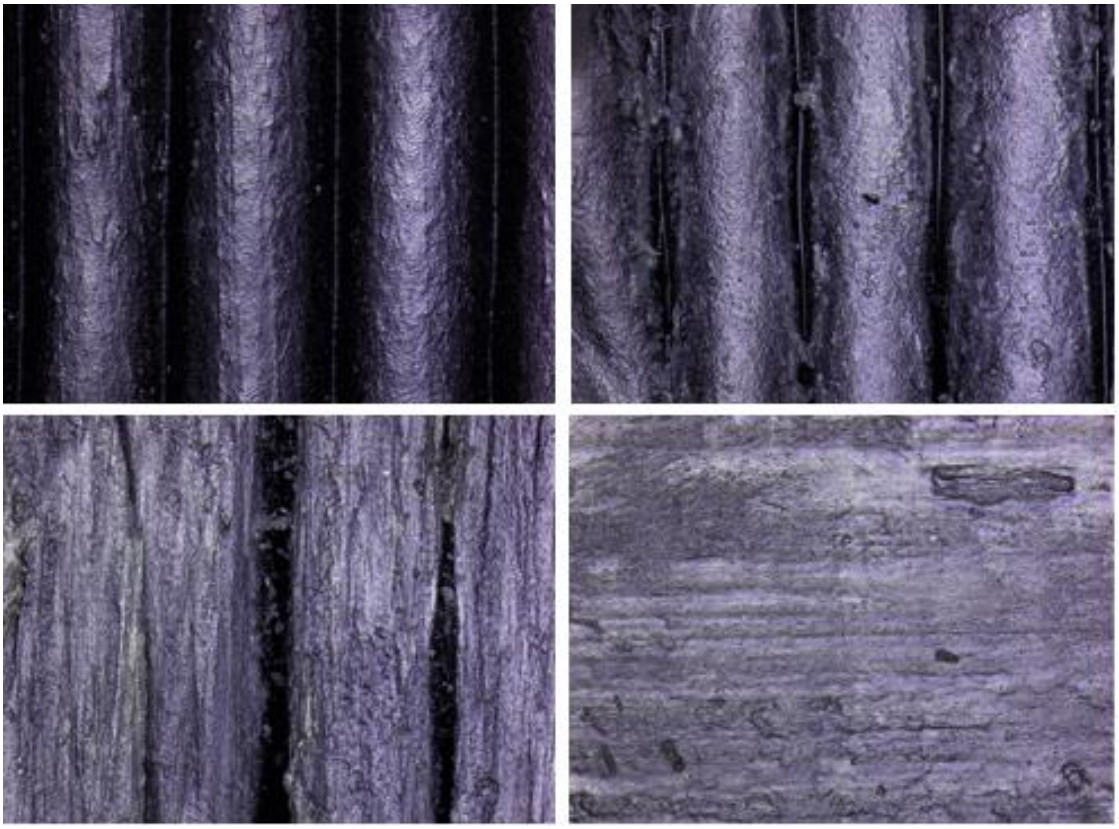

Figure 16. Microscopic pictures of LH = 0.2 mm samples. Top-left: initial; Top-right: acetone-smoothed; Bottom-left: sanded; Bottom-right: sanded/acetone-smoothed. Lens 20X.

Table 4. Surface roughness on samples with LH = 0.3 mm.

No Surface Treatments						
LH = 0.3mm	**Sample 1**	**Sample 2**	**Sample 3**			
Roughness (Ra)	28.83	27.74	27.08			
After Surface Treatment						
	Acetone 1	**Acetone 2**	**Sanding 1**	**Sanding 2**	**Sanding-Acetone 1**	**Sanding-Acetone 2**
Roughness (Ra)	22.85	20.66	3.69	4.35	1.61	1.92

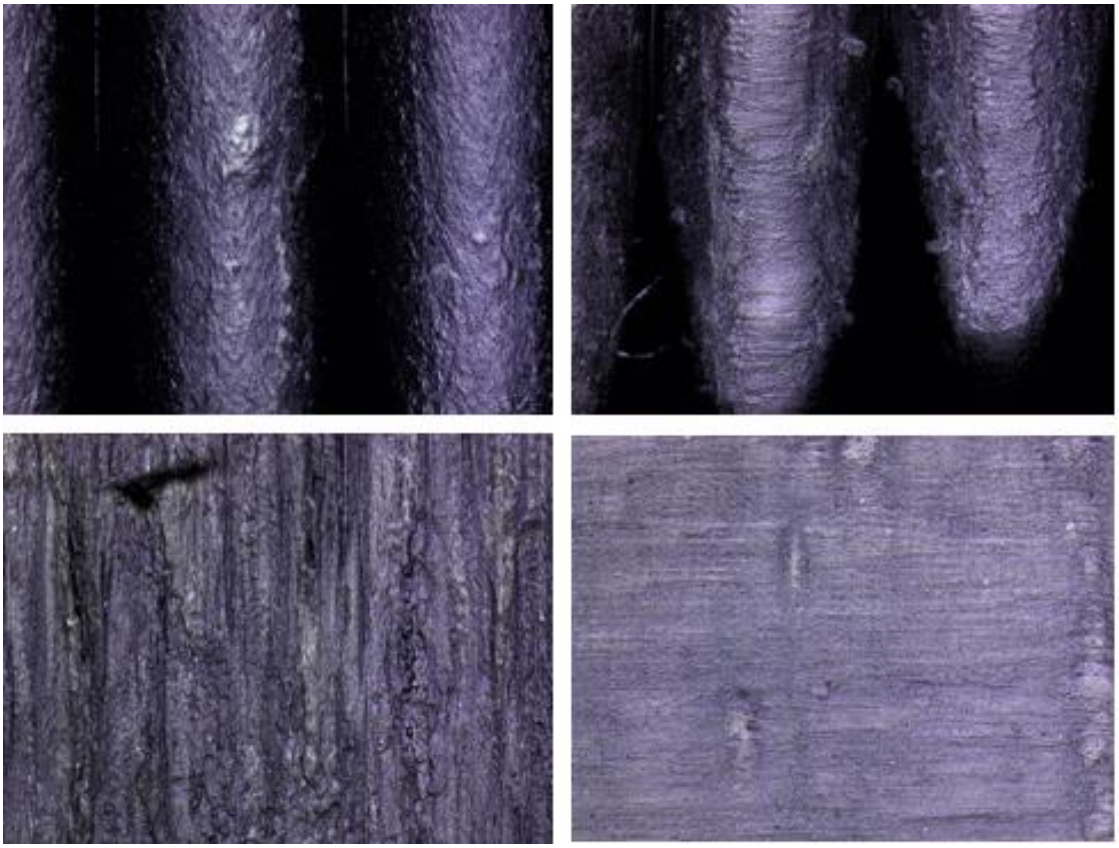

Figure 17. Microscopic pictures of LH = 0.3 mm samples. Top-left: initial; Top-right: acetone-smoothed; Bottom-left: sanded; Bottom-right: sanded/acetone-smoothed. Lens 20X.

The effects of surface roughness and printing parameters on the heat transfer coefficients with different Reynolds number were analyzed. Reynolds number represents the ratio of the inertia to viscous forces and can be calculated by Equation 7 [16], where Re represents the Reynolds number, V is the velocity of the fluid, which in this case is air, D is the diameter of the ABS cylinder, and ν is the kinematic viscosity of air.

$$\mathrm{Re} = \frac{\mathrm{VD}}{\nu} \tag{7}$$

In this first set of results, the heat transfer coeffcient and Nusselt number used are the average between all 8 locations. The following graphs show the results found for the

heat transfer coefficient and Nusselt number compared to the Reynolds number. The figures below show the graphs comparing the samples with different layer heights of 0.1 mm, 0.2 mm, and 0.3 mm.

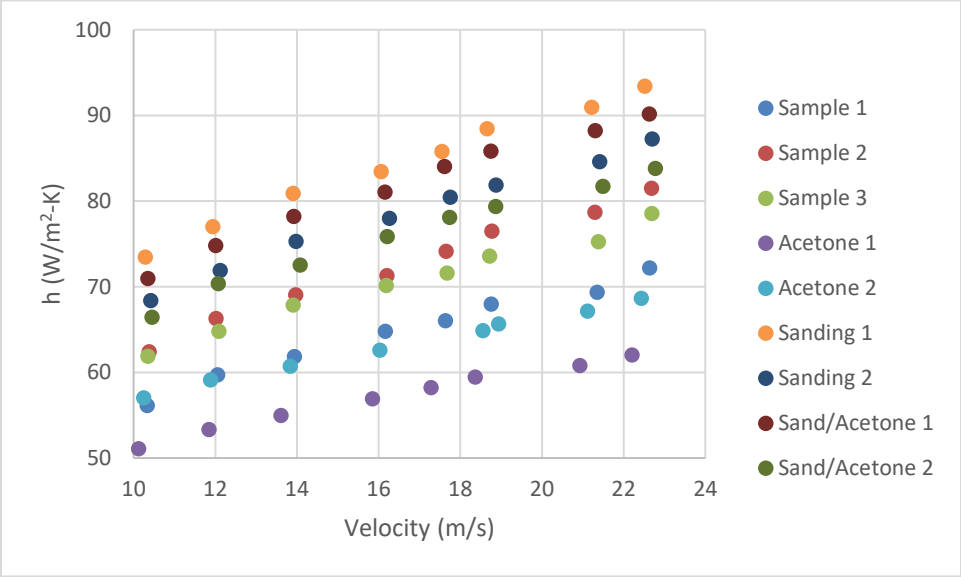

Figure 18. Dimensional heat transfer performance for different surface treatments with LH = 0.1 mm.

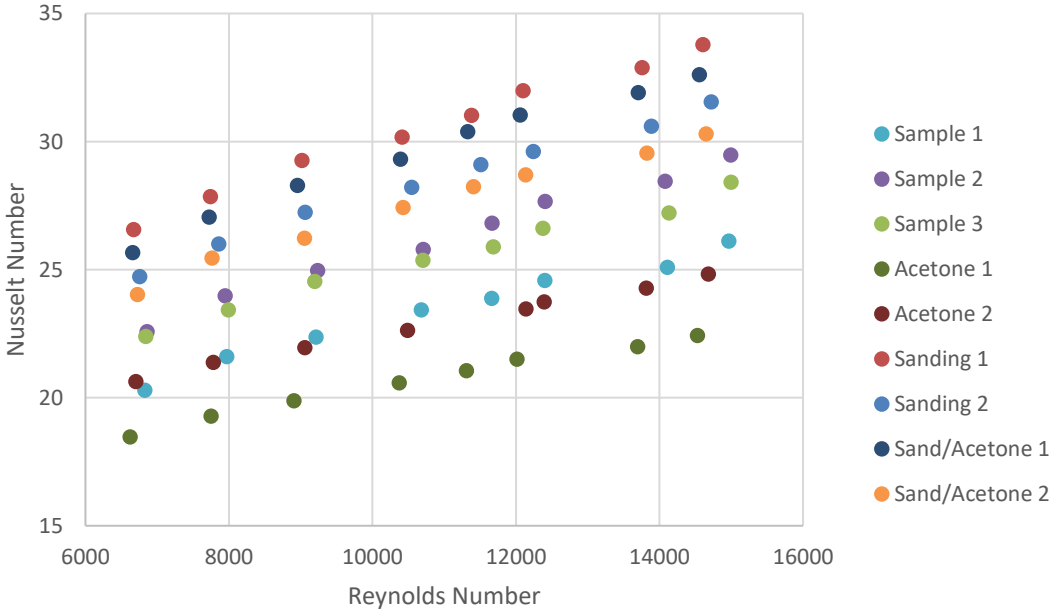

Figure 19. Nondimensional heat transfer performance for different surface treatments with LH = 0.1 mm.

After comparing and analyzing the results, the samples with layer height of 0.1 mm that achieved the highest heat transfer coefficient were the sanded and sanded/acetone-smoothed samples. The heat transfer coefficient of sanded sample 1 was 93 W/m^2-K and roughness of 4.99 µm. Sanded/acetone-smoothed sample 1 had a heat transfer coefficient value of 90 W/m^2-K and surface roughness of 1.17 µm. The sample with only acetone smoothing had the lowest value for the heat transfer coefficient: 62 W/m^2-K, with a roughness value of 9.8 µm. The samples without any alterations on the surface had a heat transfer coefficient between 72-81 W/m^2-K. All this measurements were taken at a Reynolds around 15,000. The heat transfer performance increases as the Reynolds number increases.

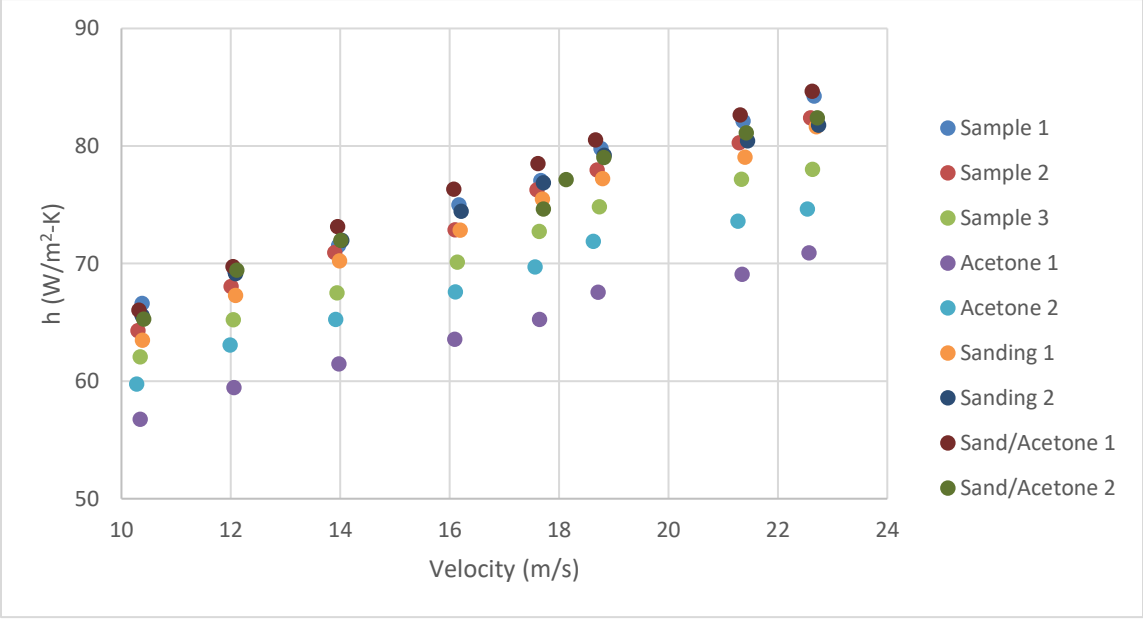

Figure 20. Dimensional heat transfer performance for different surface treatments with LH = 0.2 mm.

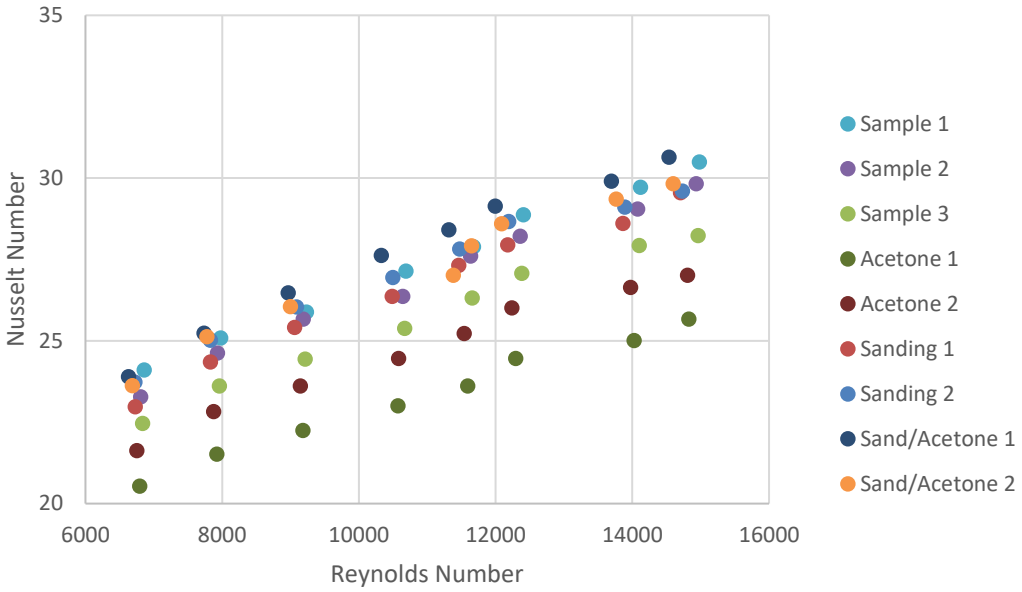

Figure 21. Nondimensional heat transfer performance for different surface treatments with LH = 0.2 mm.

The results for the samples with layer height 0.2 mm were quite different from the previous results. The highest heat transfer coefficient was a sanded/acetone-smoothed sample 1 with 85 W/m^2-K and a roughness of 1.32 μm. The samples with unchanged surfaces, sanded surfaces, and sanded/acetone-smoothed samples had similar heat transfer coefficients and the value was in between 78-85 W/m^2-K. The acetone smoothing process had a big impact with these samples. The heat transfer coefficient decreased significantly and the lowest heat transfer coefficient was 71 W/m^2-K and roughness of 11.43 μm for Acetone 1.

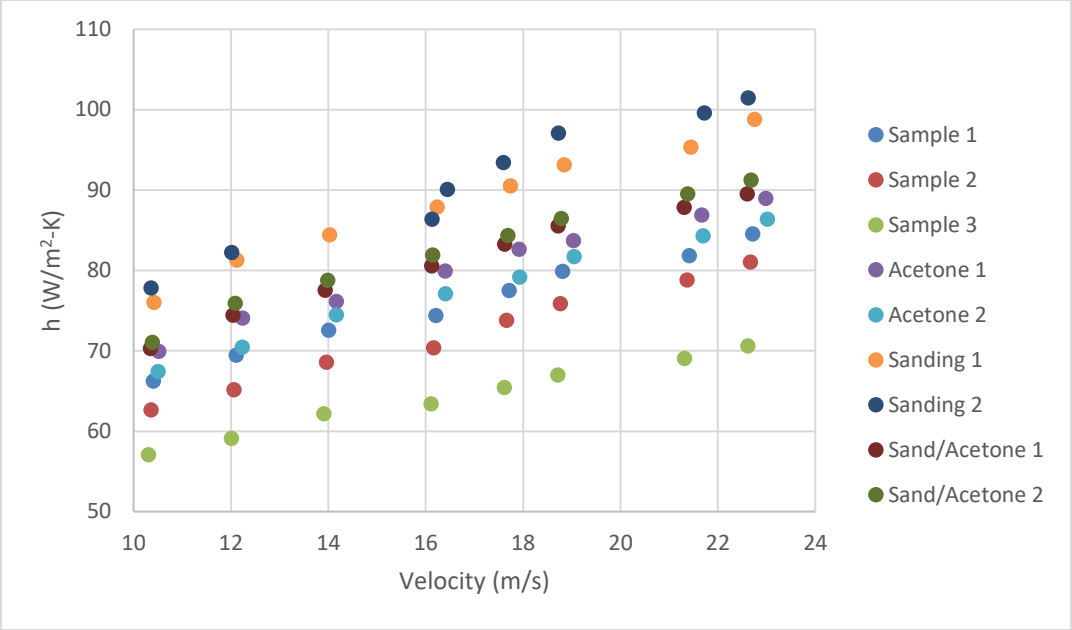

Figure 22. Dimensional heat transfer performance for different surface treatments with LH = 0.3 mm.

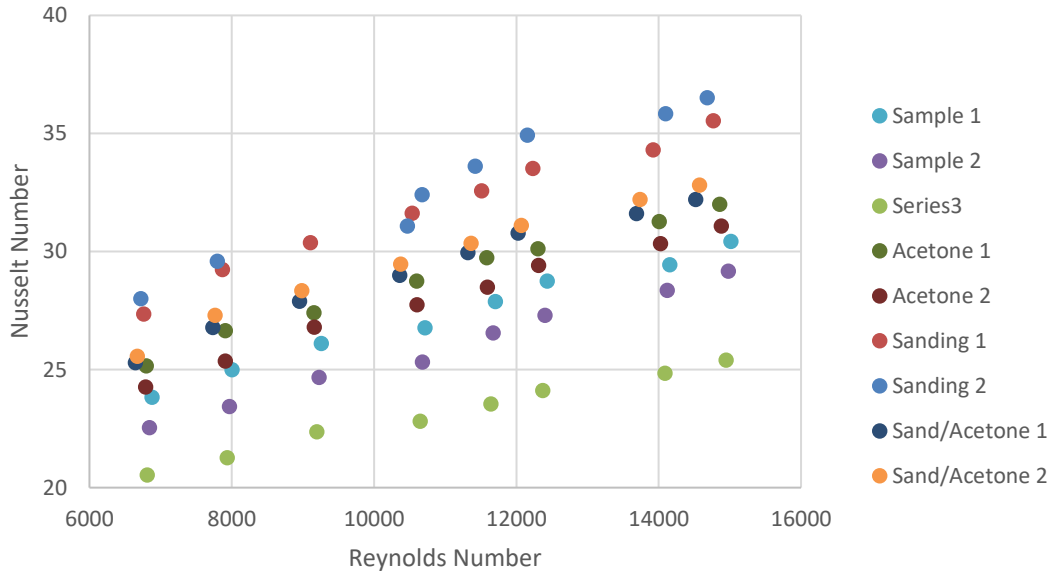

Figure 23. Nondimensional heat transfer performance for different surface treatments with LH = 0.3 mm.

The highest heat transfer coefficient found on the samples with layer height of 0.3 mm belong to the sanded sample 2 with a heat transfer coefficient of 102 W/m^2-K and a roughness of 4.35 µm. The samples with unchanged surfaces recorded the lowest values. Sample 3 recorded a heat transfer coefficient of 71 W/m^2-K and roughness of 27.08 µm.

The samples with acetone smoothed surfaces and with sanded/acetone-smoothed surfaces recorded similar heat transfer coefficient values between 86-92 W/m^2-K.

The next sets of results are divided by surface treatments. First, only the samples with the initial surface were analyzed and compared. Figure 24 illustrates the comparison. Figure 25 shows the results for only the acetone smoothed samples. Figure 26 shows the results found for only the sanded samples, and Figure 27 shows the samples that went through the sanded/acetone-smoothed process.

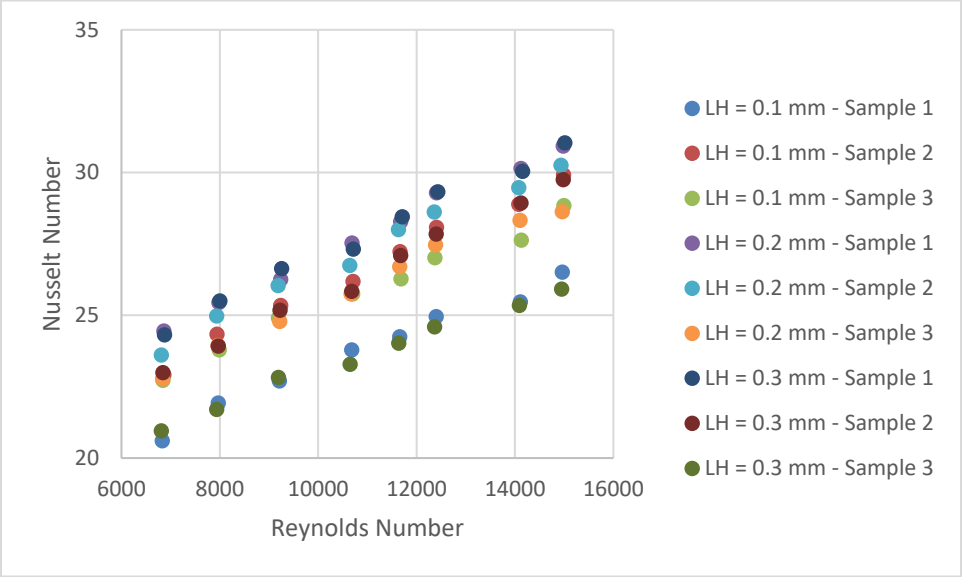

Figure 24. Nondimensional heat transfer performance for untreated surface samples.

The Nusselt number for the samples above did not vary that much, except for two samples. Sample 3 with LH = 0.3 mm, and sample 1 with LH = 0.1 mm recorded the lowest Nusselt number among all the samples with a value of 26 and 27, and roughness of 27.08 µm and 9.72 µm, respectively, at the highest Reynolds number around 15,000. The other samples recorded Nusselt number between 28-32. The difference in those two results could be explained by a misplacement of the thermocouple during testing. In order to get the

closest surface temperature, both thermocouples were placed as close as possible to the surface. However, the thermocouples for those two sample were probably placed a little below the surface. The thermocouple would read a higher temperature than the expected, which then will calculated a lower heat transfer performance. Samples with higher layer height recorded the highest Nusselt number at the highest Reynolds number around 15,000.

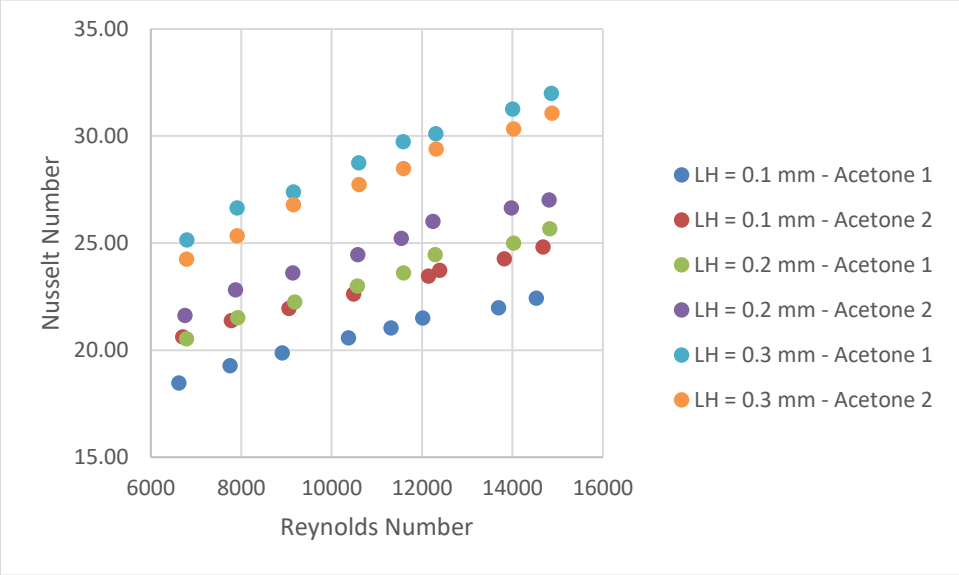

Figure 25. Nondimensional heat transfer performance for acetone smoothed samples.

The Nusselt number found for multiple samples with acetone smoothing was quite different when compared to the values with the unchanged surface samples. The samples with layer heights 0.1 mm and 0.2 mm had their Nusselt number decreased, while the samples with layer height 0.3 mm had their Nusselt number increase by smoothing it. The highest Nusselt number calculated was 33 and belong to sample 1 with LH = 0.3 mm and roughness of 22.85 µm at a Reynolds number around 15,000. The lowest Nusselt number was found to be 23, for sample 1 with LH = 0.1 mm and surface roughness of 9.8 µm at a

Reynolds number around 15,000. Decreasing the Reynolds number would also decreased the Nusselt number.

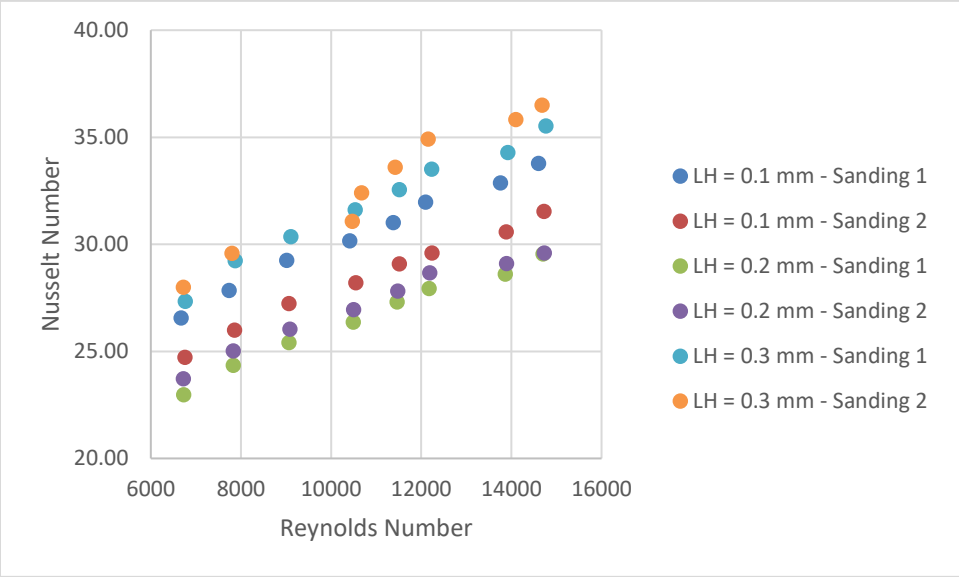

Figure 26. Nondimensional heat transfer performance for sanded samples.

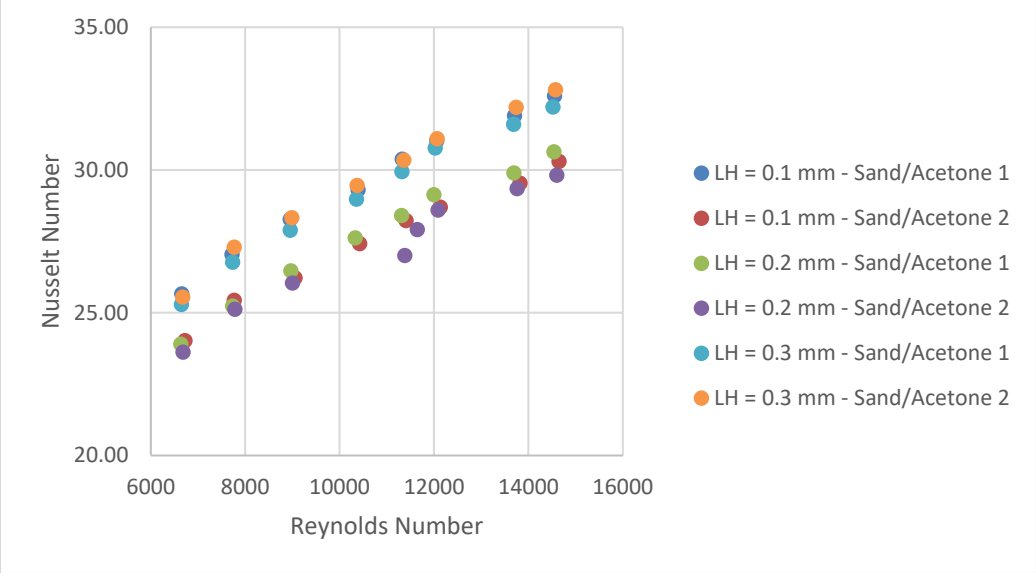

Figure 27. Nondimensional heat transfer performance for sanded/acetone-smoothed samples.

The samples that were sanded and sanded/acetone-smoothed surfaces had similar values for the Nusselt number. It varied between 29-36 at a highest Reynolds number around 15,000. In both scenarios, the samples that were printed with a LH = 0.3 mm had the highest Nusselt numbers, such as Nu = 33, roughness 4.35 μm for sanded, and Nu = 36, roughness 1.92 μm for sanded/acetone-smoothed samples. Also, the samples with LH = 0.2 mm had the lowest Nusselt number, such as Nu = 29, roughness 3.26 μm for sanded samples, and Nu = 30, roughness of 1.19 μm for sanded/acetone-smoothed samples.

DISCUSSION

Samples with a layer height of 0.1 mm had the smallest surface roughness and recorded the lowest heat transfer coefficient and Nusselt number at the highest Reynolds number around 15,000. Samples with no surface treatment recorded Nusselt number between 26-31. After the acetone treatment, the roughness did not see a big change, it barely went down by 1 μm, but the Nusselt number decreased. Sanding and sanding/acetone-smoothing treatments reduced the surface roughness significantly, while increasing the Nusselt number. In this scenario the roughness decreased from around 10 μm to 4 μm for sanded samples and to 1 μm to sanded/acetone-smoothing samples.

Samples with LH = 0.2 mm with no surface treatment were rougher compared to the 0.1 mm samples and had a calculated Nusselt number between 23-32 at the highest Reynolds number. The acetone treatment reduced the roughness by the largest amount in this layer height, reducing the roughness by more than 10 μm. The Nusselt number calculated at the highest Reynolds number was smaller when compared to the untreated surface samples, Nu = 26 for the acetone samples and Nu = 31 for the untreated surface samples. Even though sanding and sanding/acetone-smoothing treatments reduced the surface roughness drastically to around 3 μm and 1 μm respectively, the Nusselt number was similar to the untreated surface samples.

Samples with LH = 0.3 mm had the highest surface roughness and recorded the highest Nusselt number. After the surface treatment, the acetone smoothing samples had different results when compared to the lower layer heights. The roughness reduced by 6-7 μm, however, the Nusselt number was essentially unchanged. The sanding and acetone-smoothing/sanding treatments follow the same pattern as the lower layer heights, reducing

the roughness, while increasing the Nusselt number. The roughness values were reduced by close to 25 μm for sanded samples and reduced by 27 μm for sanded/acetone-smoothing samples and the Nusselt number increased in both cases. For example, untreated surface sample 2 with a roughness of 27.74 μm had a Nusselt number around 29. After the sanding treatment, the surface roughness was 4.35 μm and a Nusselt number around 36. After the sanding treatment, the surface roughness was 1.92 μm and a Nusselt number around 33.

The calculated Nusselt number for the samples with untreated surface was between 26-31. Lower layer heights recorded the smallest roughness value and with the increase in layer height, roughness also increased. After the surface treatment, samples with different layer heights had different responses to the same surface treatment. The roughness was reduced on all three treatments. Among the acetone samples, the samples with lower layer height had their Nusselt number reduced, while at LH = 0.3 mm the Nusselt number had a slightly increase. In addition, the acetone treatment reduced the roughness by different amounts for each layer height. Samples printed with LH = 0.1 mm had a decrease in roughness around 1 μm while samples with a LH = 0.3 had a decrease in roughness around 6-7 μm. The biggest reduction in roughness occurred with samples with a LH = 0.2 mm, the roughness decreased by 10-11 μm. The sanded samples recorded an even smaller surface roughness. However, the Nusselt number increased in this scenario. The same situation happened for the sanded/acetone-smoothed samples, but because acetone was added, the roughness and thermal performance decreased by a small factor when comparing to the sanded samples, but still getting a high Nusselt number. The main reason is that the sanding process changed the character of roughness of the surface. Figure 28 illustrates the change. Initially, the character of roughness had a wave profile in which the

width of each wave is the layer height. As the figure shows, acetone smoothing did not change the roughness profile by much. However, sanding changed significantly the character of roughness. The roughness profile does not resemble each layer anymore. The profile is straight with some small variations but made of a large amount of smaller waves. This new profile show an increase in the surface area where the convective heat transfer is occurring. Surface area is directly proportional to the heat transfer performance, therefore, increasing the area it would also increase the heat transfer coefficient.

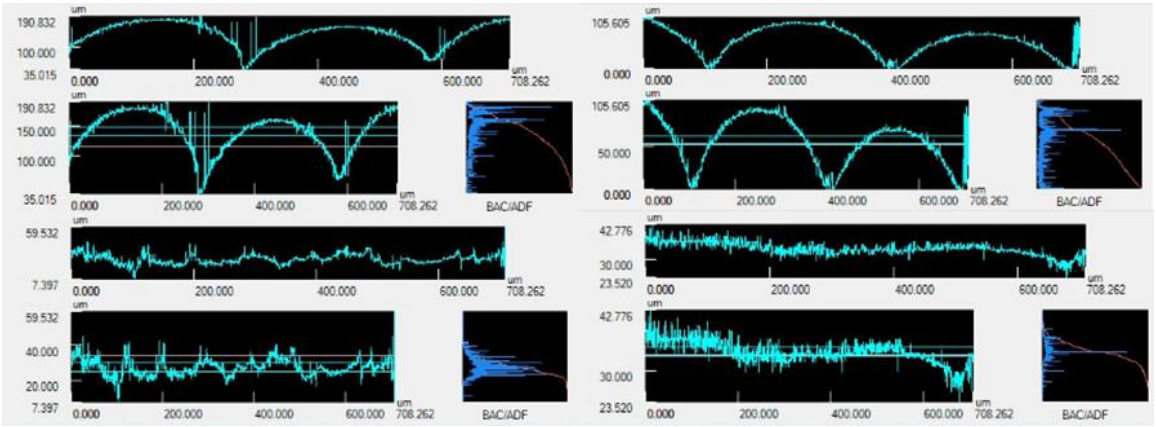

Figure 28. Character of roughness for different surface treatments. Top-left: no surface treatment; top-right: acetone smoothing; bottom-left: sanding; bottom-right: sanding/acetone.

After the sanding and sanding/acetone treatments, it was interesting to see that the samples with different layer heights started with different surface roughness and at the end of each treatment, all samples had a similar surface roughness. After the sanding treatments, all samples had a surface roughness around 3-5 µm and after sanding/acetone treatments the roughness was reduced to 1-2 µm. Since the roughness is similar among all samples, it would be expected that they would also have similar heat transfer performance. The sanding/acetone samples follow this pattern, where both sample with LH = 0.3 mm, roughness of 1.61 µm and 1.92 µm and one sample with LH = 0.1 mm, roughness of 1.17,

had a calculated Nusselt number around 33. The other sample with LH =0.1 mm, roughness of 0.85 µm and both samples printed with LH = 0.2 mm, roughness of 1.32 µm and 1.19 µm had a similar Nusselt number around 30. However, even though the sanding sample ended up with similar surface roughness, the heat transfer performance varied with the different layer heights. Samples with LH = 0.3, had a surface roughness of 3.69 µm and 4.35 µm and had the highest Nusselt number around 36 at the highest Reynolds number. Samples with LH = 0.2, had a surface roughness of 3.26 µm and 33 µm and had the lowest Nusselt number around 29.

CONCLUSIONS

The effects of surface roughness on heat transfer of a 3d printed part was analyzed. Layer heights of 0.1 mm, 0.2 mm, and 0.3 mm were used in combination with surface treatments of acetone smoothing, sanding, and sanding/acetone-smoothing to create different roughness values. After recording surface roughness profiles, the heat transfer coefficient and Nusselt number values were found.

Samples with different printing parameters were analyzed first. As the layer height increases, the heat transfer coefficient recorded increased. After the surface treatment, samples were affected differently. Acetone had a different impact at different layer heights. At lower layer heights, roughness was reduced and the heat transfer performance decreased, while at a higher layer height roughness was also reduced, but the heat transfer performance improved. The sanding and sanding/acetone-smoothing had the opposite impact. Higher layer heights were affected more. In this process, the heat transfer coefficient increased, even though the roughness was reduced. The sanding process changed the character of roughness by extracting material until the wave profile changed to a smother line.

After analyzing and comparing the results, it has been shown that a 3d printed part can have higher convective heat transfer with some surface treatment. If the part is designed to prevent heat from coming and going, an acetone smoothing treatment is ideal because of it would reduce the heat transfer coefficient. However, if the part is designed to dissipate heat, a sanding treatment is ideal. It reduces the surface roughness while increasing the heat transfer coefficient. Also, since the sanding process was more effective on high layer height, a high layer height should be used. Manufacturing parts with a higher layer height

reduces cost, printing time, and it can improve the mechanical performance, but is not visually appealing for the printed part. The sanding process can adjust that issue by smoothing to the best look. However, it can be difficult to sand complex designs.

The work performed in this thesis was limited to ABS cylinder samples and certain surface treatments. Further investigation into different polymers would provide data that could be compared to the ABS samples. The surface treatments could affect the heat transfer differently in different materials. Also, printing and testing an ABS heat exchangers would show how feasible or not to it is to print the part with different layer heights and perform different surface treatments.

REFERENCES

[1] Ngo, T. D., Kashani, A., Imbalzano, G., Nguyen, K. T., & Hui, D. (n.d.). Additive Manufacturing (3D printing): A review of material, methods, applications and challenges.

[2] Ligon, S. C., Liska, R., Stampfl, J., Gurr, M., & Muelhaupt, R. (2017). Polymers for 3D Printing and Customized Additive Manufacturing. Chemical Reviews, 117(15), 10212-10290.

[3] Arie, Martinus A. et al. Experimental Characterization of Heat Transfer In an Additively Manufactured Polymer Heat Exchanger. Applied Thermal Engineering, vol 113, 2017, pp. 575-584.

[4] Michna, G. J., & Letcher, T. (2018, June), Designing 3-D Printed Heat Exchangers in a Senior-level Thermal Systems Course Paper presented at 2018 ASEE Annual Conference & Exposition , Salt Lake City, Utah. https://peer.asee.org/30274

[5] Felber, R. A., Nellis, G., & Rudolph, N. (2016). Design and Modeling of 3D-Printed Air-Cooled Heat Exchangers. International Refrigeration and Air Conditioning Conference.

[6] Wu, P., & Lttle, W. A. (1984). Measurement of the Heat Transfer Characteristics of Gas Flow in Fine Channel Heat Exchangers Used for Micro-miniature Refrigerators.

[7] Maisurua, Mahendrakumar. Effect of Surface Roughness on Heat Transfer.

[8] Achenbach, E. (1968). Distribution of local pressure and skin friction around a circular cylinder in cross-flow up to Re = 5 × 10 6. Journal of Fluid Mechanics, 34(04), p.625.

[9] Achenbach, E. (1971). Influence of surface roughness on the cross-flow around a circular cylinder. Journal of Fluid Mechanics, v46, part2, pp. 321-335.

[10] Everts, M., Ayres, S. R., Houwer, F. A., Vanderwagen, C. P., Kotze, N. M., & Meyer, J. P. (2014). The Influence of Surface Roughness on Heat Transfer in the Transitional Flow Regime. Proceedings of the 15th International Heat Transfer Conference. doi:10.1615/ihtc15.cnv.008338

[11] Zhang, C., Chen, Y., & Shi, M. (2010). Effects of roughness elements on laminar flow and heat transfer in microchannels. Chemical Engineering and Processing: Process Intensification, 49(11), 1188-1192. doi:10.1016/j.cep.2010.08.022

[12] Wu, H., & Cheng, P. (2003). An experimental study of convective heat transfer in silicon microchannels with different surface conditions. International Journal of Heat and Mass Transfer, 46(14), 2547-2556. doi: 10.1016/s0017-9310(03)00035-8.

[13] Dierich, F., & Niktrityuk, P. (2013). A numerical study of the impact of surface roughness on heat and fluid flow past a cylindrical particle. International Journal of Thermal Sciences, 65, 92-103. doi: 1-.1016/j.ijthermalsci.2012.09.009

[14] Kandlikar, S. G., Joshi, S., & Tian, S. (2003). Effect of Surface Roughness on Heat Transfer and Fluid Flow Characteristics at Low Reynolds Numbers in Small Diameter Tubes. Heat Transfer Engineering, 24(3), 4-16. Doi: 10.1080/01457630304069

[15] Cain, P. (n.d.). The Impact of Layer Height on a 3D Print. Retrieved from https://www.3dhubs.com/knowledge-base/impact-layer-height-3d-print

[16] Incropera, F. P., Dewitt, D. P., Bergman, T. L., & Lavine, A. S. (2007). Fundamentals of Heat and Mass Transfer (6th Ed.). Hoboken, NJ: John Wiley & Sons.

[17] Kline, S. J., & McClintock, F. A. (1953). Describing Uncertainties in Single-Sample Experiments.

APPENDICES

Appendix A: Experimental data collected by LabView.

Temp 0	Temp 1	Temp 2	Temp 3	Temp 4	Temp 5	Temp 6	Temp 7	Temp 8	V	I
21.45	21.74	21.78	21.69	21.82	21.82	21.85	56.05	57.64	0.98	0.17
21.44	21.72	21.75	21.67	21.79	21.81	21.83	56.05	57.65	0.98	0.17
21.44	21.77	21.75	21.66	21.81	21.83	21.82	56.06	57.65	0.98	0.17
21.44	21.79	21.74	21.65	21.81	21.82	21.82	56.06	57.66	0.98	0.17
21.44	21.79	21.76	21.66	21.82	21.83	21.81	56.07	57.67	0.98	0.17
21.44	21.78	21.76	21.67	21.82	21.82	21.83	56.07	57.67	0.98	0.17
21.44	21.82	21.77	21.68	21.85	21.84	21.84	56.08	57.69	0.98	0.17
21.44	21.81	21.79	21.72	21.85	21.84	21.88	56.08	57.71	0.98	0.17
21.44	21.80	21.78	21.69	21.83	21.84	21.84	56.09	57.72	0.98	0.17
21.44	21.80	21.79	21.62	21.85	21.83	21.81	56.10	57.72	0.98	0.17
21.44	21.81	21.78	21.59	21.84	21.82	21.80	56.11	57.73	0.98	0.17
21.44	21.81	21.77	21.66	21.85	21.84	21.85	56.12	57.74	0.98	0.17
21.44	21.80	21.80	21.72	21.84	21.87	21.89	56.12	57.74	0.98	0.17
21.44	21.77	21.77	21.76	21.81	21.84	21.90	56.13	57.75	0.98	0.17
21.44	21.76	21.73	21.72	21.81	21.82	21.87	56.13	57.76	0.98	0.17
21.44	21.77	21.79	21.75	21.83	21.87	21.92	56.14	57.76	0.98	0.17
21.44	21.84	21.88	21.83	21.87	21.94	21.97	56.14	57.77	0.98	0.17
21.44	21.86	21.89	21.78	21.90	21.94	21.94	56.15	57.77	0.98	0.17
21.44	21.87	21.90	21.79	21.90	21.94	21.95	56.16	57.79	0.98	0.17
21.44	21.86	21.88	21.81	21.90	21.93	21.95	56.16	57.79	0.98	0.17
21.44	21.83	21.87	21.83	21.89	21.93	21.96	56.17	57.81	0.98	0.17
21.44	21.81	21.90	21.81	21.89	21.93	21.95	56.18	57.82	0.98	0.17
21.44	21.77	21.89	21.82	21.87	21.92	21.97	56.18	57.82	0.98	0.17
21.44	21.78	21.85	21.82	21.86	21.92	21.97	56.19	57.83	0.98	0.17
21.44	21.77	21.84	21.81	21.84	21.91	21.95	56.19	57.84	0.98	0.17
21.44	21.84	21.86	21.79	21.89	21.90	21.95	56.18	57.84	0.98	0.17
21.44	21.86	21.84	21.77	21.90	21.89	21.93	56.20	57.84	0.98	0.17
21.44	21.84	21.83	21.78	21.88	21.90	21.93	56.21	57.85	0.98	0.17
21.44	21.79	21.80	21.79	21.86	21.87	21.91	56.21	57.85	0.98	0.17
21.44	21.77	21.80	21.74	21.84	21.86	21.90	56.21	57.86	0.98	0.17
21.44	21.75	21.77	21.72	21.81	21.84	21.90	56.23	57.87	0.98	0.17
21.44	21.75	21.78	21.72	21.82	21.84	21.89	56.23	57.87	0.98	0.17
21.44	21.76	21.77	21.77	21.83	21.83	21.90	56.23	57.86	0.98	0.17
21.44	21.78	21.73	21.77	21.83	21.79	21.88	56.22	57.86	0.98	0.17
21.44	21.74	21.73	21.80	21.82	21.82	21.92	56.22	57.87	0.98	0.17

21.44	21.80	21.82	21.82	21.87	21.88	21.95	56.23	57.88	0.98	0.17
21.44	21.80	21.81	21.80	21.87	21.89	21.95	56.23	57.88	0.98	0.17
21.44	21.80	21.84	21.82	21.87	21.91	21.97	56.25	57.89	0.98	0.17
21.44	21.78	21.83	21.80	21.85	21.90	21.95	56.25	57.89	0.98	0.17
21.44	21.78	21.82	21.77	21.85	21.87	21.92	56.24	57.89	0.98	0.17
21.44	21.78	21.81	21.77	21.86	21.86	21.92	56.25	57.90	0.98	0.17
21.44	21.80	21.80	21.76	21.88	21.87	21.93	56.26	57.90	0.98	0.17
21.44	21.81	21.85	21.76	21.88	21.91	21.94	56.27	57.91	0.98	0.17
21.44	21.81	21.86	21.78	21.86	21.92	21.95	56.27	57.92	0.98	0.17
21.44	21.82	21.86	21.79	21.88	21.93	21.95	56.28	57.95	0.98	0.17
21.44	21.85	21.87	21.78	21.91	21.94	21.95	56.28	57.95	0.98	0.17
21.44	21.88	21.88	21.79	21.92	21.94	21.96	56.29	57.94	0.98	0.17
21.44	21.88	21.85	21.76	21.91	21.90	21.93	56.29	57.94	0.98	0.17
21.44	21.85	21.82	21.70	21.90	21.87	21.89	56.29	57.95	0.98	0.17
21.44	21.91	21.84	21.74	21.94	21.91	21.92	56.29	57.96	0.98	0.17
21.44	21.91	21.89	21.81	21.94	21.95	21.97	56.30	57.96	0.98	0.17
21.44	21.87	21.89	21.81	21.92	21.94	21.96	56.30	57.97	0.98	0.17
21.44	21.84	21.89	21.83	21.89	21.96	21.99	56.31	57.97	0.98	0.17
21.44	21.85	21.91	21.88	21.91	21.99	22.03	56.31	57.97	0.98	0.17
21.44	21.91	21.94	21.87	21.96	21.99	22.01	56.32	57.98	0.98	0.17
21.44	21.94	21.95	21.84	21.97	21.99	21.99	56.34	58.00	0.98	0.17
21.44	21.92	21.93	21.82	21.96	21.98	21.98	56.34	58.00	0.98	0.17
21.44	21.92	21.93	21.83	21.97	21.97	22.00	56.34	58.01	0.98	0.17
21.44	21.94	21.96	21.84	22.00	22.00	22.00	56.35	58.03	0.98	0.17
21.44	21.92	21.93	21.83	21.97	21.99	21.99	56.36	58.03	0.98	0.17
21.44	21.90	21.91	21.84	21.94	21.97	21.99	56.36	58.04	0.98	0.17
21.44	21.90	21.91	21.82	21.95	21.96	21.97	56.37	58.06	0.98	0.17
21.44	21.91	21.92	21.81	21.95	21.96	21.97	56.38	58.07	0.98	0.17
21.44	21.82	21.88	21.81	21.90	21.93	21.97	56.38	58.06	0.98	0.17
21.44	21.86	21.89	21.81	21.91	21.93	21.96	56.38	58.07	0.98	0.17
21.44	21.85	21.86	21.79	21.90	21.91	21.94	56.37	58.07	0.98	0.17
21.44	21.84	21.82	21.76	21.88	21.88	21.92	56.38	58.08	0.98	0.17
21.44	21.84	21.83	21.78	21.88	21.89	21.92	56.39	58.10	0.98	0.17
21.44	21.83	21.82	21.80	21.87	21.89	21.95	56.39	58.10	0.98	0.17
21.44	21.83	21.83	21.79	21.88	21.90	21.95	56.39	58.11	0.98	0.17
21.44	21.83	21.85	21.82	21.90	21.92	21.97	56.39	58.11	0.98	0.17
21.44	21.86	21.86	21.86	21.91	21.93	22.01	56.39	58.11	0.98	0.17
21.44	21.87	21.89	21.86	21.93	21.95	22.01	56.40	58.11	0.98	0.17
21.44	21.87	21.92	21.90	21.95	21.97	22.04	56.40	58.11	0.98	0.17
21.44	21.90	21.94	21.93	21.96	21.99	22.06	56.41	58.11	0.98	0.17
21.44	21.90	21.94	21.90	21.95	21.99	22.04	56.42	58.12	0.98	0.17

21.44	21.90	21.92	21.84	21.96	21.97	22.01	56.42	58.12	0.98	0.17
21.44	21.90	21.93	21.87	21.96	21.98	22.02	56.42	58.11	0.98	0.17
21.44	21.91	21.94	21.88	21.96	21.99	22.02	56.42	58.12	0.98	0.17
21.44	21.90	21.94	21.89	21.96	21.99	22.04	56.43	58.13	0.98	0.17
21.44	21.87	21.92	21.87	21.93	21.97	22.02	56.42	58.14	0.98	0.17
21.44	21.86	21.92	21.83	21.93	21.96	21.98	56.42	58.15	0.98	0.17
21.44	21.87	21.88	21.85	21.92	21.95	22.00	56.43	58.14	0.98	0.17
21.44	21.86	21.88	21.87	21.92	21.96	22.01	56.43	58.14	0.98	0.17
21.44	21.88	21.90	21.87	21.94	21.98	22.03	56.43	58.15	0.98	0.17
21.44	21.87	21.92	21.87	21.92	21.98	22.03	56.44	58.15	0.98	0.17
21.44	21.85	21.91	21.86	21.90	21.98	22.01	56.44	58.15	0.98	0.17
21.44	21.88	21.88	21.84	21.92	21.95	22.00	56.45	58.16	0.98	0.17
21.44	21.89	21.90	21.85	21.93	21.95	22.02	56.44	58.16	0.98	0.17
21.44	21.87	21.87	21.87	21.91	21.95	22.02	56.44	58.16	0.98	0.17
21.44	21.89	21.89	21.84	21.93	21.97	22.00	56.46	58.17	0.98	0.17
21.44	21.89	21.92	21.82	21.93	21.97	21.98	56.45	58.16	0.98	0.17
21.44	21.89	21.91	21.82	21.95	21.95	21.98	56.45	58.17	0.98	0.17
21.44	21.88	21.90	21.82	21.94	21.94	21.97	56.45	58.17	0.98	0.17
21.44	21.86	21.88	21.81	21.92	21.94	21.96	56.45	58.17	0.98	0.17
21.44	21.79	21.84	21.79	21.86	21.89	21.94	56.45	58.17	0.98	0.17
21.44	21.86	21.85	21.78	21.90	21.91	21.94	56.47	58.19	0.98	0.17
21.44	21.87	21.86	21.79	21.90	21.91	21.95	56.46	58.18	0.98	0.17
21.44	21.88	21.88	21.81	21.93	21.92	21.99	56.45	58.17	0.98	0.17
21.44	21.88	21.89	21.83	21.94	21.92	21.99	56.45	58.17	0.98	0.17
21.44	21.91	21.91	21.86	21.96	21.96	22.02	56.47	58.18	0.98	0.17
21.44	21.89	21.92	21.88	21.94	21.98	22.03	56.47	58.18	0.98	0.17
21.44	21.87	21.91	21.87	21.93	21.98	22.02	56.48	58.19	0.98	0.17
21.44	21.87	21.93	21.88	21.93	22.00	22.03	56.48	58.20	0.98	0.17
21.44	21.90	21.94	21.89	21.95	22.01	22.03	56.48	58.21	0.98	0.17
21.44	21.90	21.95	21.86	21.96	21.99	22.02	56.48	58.20	0.98	0.17
21.44	21.92	21.93	21.87	21.96	21.99	22.02	56.49	58.20	0.98	0.17
21.44	21.94	21.95	21.88	21.97	22.01	22.03	56.50	58.20	0.98	0.17
21.44	21.97	21.97	21.88	22.01	22.01	22.03	56.50	58.22	0.98	0.17
21.44	21.96	21.96	21.89	21.99	22.00	22.03	56.49	58.21	0.98	0.17
21.44	21.95	21.95	21.89	21.99	22.00	22.03	56.49	58.22	0.98	0.17
21.44	21.94	21.96	21.89	21.99	22.01	22.04	56.50	58.22	0.98	0.17
21.44	21.94	21.98	21.89	21.99	22.03	22.05	56.50	58.23	0.98	0.17
21.44	21.94	21.97	21.94	21.99	22.03	22.10	56.51	58.22	0.98	0.17
21.44	21.93	21.97	21.95	21.99	22.03	22.10	56.50	58.23	0.98	0.17
21.44	21.91	21.95	21.93	21.97	22.01	22.07	56.52	58.25	0.98	0.17
21.44	21.90	21.94	21.91	21.96	22.02	22.06	56.53	58.25	0.98	0.17

21.44	21.90	21.99	21.93	21.97	22.04	22.08	56.53	58.25	0.98	0.17
21.44	21.93	22.00	21.95	21.99	22.06	22.10	56.53	58.27	0.98	0.17
21.44	21.94	22.01	21.93	22.00	22.06	22.08	56.52	58.27	0.98	0.17
21.44	21.95	22.00	21.94	22.01	22.05	22.08	56.54	58.28	0.98	0.17
21.44	21.95	21.98	21.93	22.00	22.04	22.07	56.55	58.29	0.98	0.17
21.44	21.93	21.96	21.92	21.98	22.02	22.06	56.55	58.29	0.98	0.17
21.44	21.93	21.95	21.90	21.97	22.01	22.04	56.55	58.29	0.98	0.17
21.44	21.90	21.94	21.89	21.96	21.99	22.03	56.55	58.30	0.98	0.17
21.44	21.87	21.92	21.89	21.92	21.96	22.03	56.56	58.30	0.98	0.17
21.44	21.87	21.91	21.89	21.92	21.97	22.04	56.56	58.30	0.98	0.17
21.44	21.89	21.91	21.88	21.94	21.97	22.04	56.56	58.31	0.98	0.17
21.44	21.87	21.92	21.90	21.93	21.99	22.05	56.57	58.32	0.98	0.17
21.44	21.84	21.88	21.92	21.89	21.97	22.05	56.58	58.32	0.98	0.17
21.44	21.84	21.89	21.91	21.90	21.97	22.06	56.56	58.31	0.98	0.17
21.44	21.90	21.91	21.93	21.94	21.97	22.07	56.56	58.31	0.98	0.17
21.44	21.93	21.96	21.94	21.99	22.02	22.07	56.58	58.32	0.98	0.17
21.44	21.93	21.94	21.93	21.97	22.03	22.07	56.58	58.32	0.98	0.17
21.44	21.92	21.93	21.92	21.97	22.02	22.06	56.59	58.34	0.98	0.17
21.44	21.89	21.94	21.91	21.95	22.02	22.06	56.58	58.33	0.98	0.17
21.44	21.88	21.93	21.89	21.94	21.98	22.03	56.58	58.33	0.98	0.17
21.44	21.89	21.91	21.88	21.95	21.96	22.02	56.58	58.33	0.98	0.17
21.44	21.87	21.94	21.87	21.95	21.97	22.02	56.59	58.34	0.98	0.17
21.44	21.89	21.93	21.84	21.95	21.98	22.00	56.59	58.34	0.98	0.17
21.44	21.89	21.91	21.84	21.95	21.96	22.00	56.58	58.34	0.98	0.17
21.44	21.89	21.91	21.84	21.95	21.97	22.00	56.58	58.34	0.98	0.17
21.44	21.91	21.94	21.89	21.97	22.01	22.03	56.58	58.35	0.98	0.17
21.44	21.92	21.95	21.90	21.97	22.01	22.04	56.59	58.35	0.98	0.17
21.44	21.92	21.92	21.88	21.96	21.97	22.03	56.59	58.35	0.98	0.17
21.44	21.91	21.92	21.82	21.96	21.97	21.99	56.58	58.35	0.98	0.17
21.44	21.88	21.90	21.79	21.92	21.93	21.96	56.59	58.35	0.98	0.17
21.44	21.82	21.85	21.87	21.87	21.95	22.01	56.60	58.36	0.98	0.17
21.44	21.87	21.92	21.90	21.94	22.01	22.05	56.60	58.37	0.98	0.17
21.44	21.89	21.95	21.91	21.95	22.02	22.06	56.61	58.37	0.98	0.17
21.44	21.86	21.92	21.90	21.91	21.99	22.05	56.61	58.37	0.98	0.17
21.44	21.82	21.88	21.89	21.89	21.95	22.01	56.60	58.36	0.98	0.17
21.44	21.81	21.88	21.82	21.89	21.93	22.00	56.60	58.36	0.98	0.17
21.44	21.87	21.91	21.88	21.94	21.98	22.04	56.61	58.36	0.98	0.17
21.44	21.93	21.95	21.87	21.98	22.01	22.03	56.62	58.37	0.98	0.17
21.44	21.92	21.94	21.84	21.96	22.00	22.00	56.62	58.38	0.98	0.17
21.44	21.89	21.90	21.84	21.94	21.96	21.99	56.62	58.38	0.98	0.17
21.44	21.88	21.91	21.86	21.93	21.95	22.02	56.63	58.38	0.98	0.17

21.44	21.88	21.91	21.87	21.93	21.96	22.03	56.63	58.37	0.98	0.17
21.44	21.91	21.91	21.86	21.94	21.97	22.03	56.62	58.38	0.98	0.17
21.44	21.91	21.93	21.87	21.95	21.99	22.03	56.64	58.37	0.98	0.17
21.44	21.91	21.90	21.86	21.94	21.96	22.01	56.64	58.39	0.98	0.17
21.44	21.90	21.83	21.86	21.92	21.94	22.01	56.64	58.40	0.98	0.17
21.44	21.87	21.89	21.89	21.91	21.97	22.04	56.64	58.40	0.98	0.17
21.44	21.88	21.95	21.91	21.95	22.02	22.06	56.64	58.40	0.98	0.17
21.44	21.90	21.97	21.92	21.96	22.02	22.07	56.64	58.39	0.98	0.17
21.44	21.92	21.98	21.92	21.98	22.04	22.07	56.66	58.41	0.98	0.17
21.44	21.91	21.96	21.90	21.96	22.02	22.06	56.65	58.40	0.98	0.17
21.44	21.93	21.95	21.89	21.98	22.00	22.04	56.65	58.41	0.98	0.17
21.44	21.96	21.96	21.86	22.00	22.02	22.03	56.65	58.41	0.98	0.17
21.44	21.92	21.95	21.84	21.97	22.00	22.01	56.66	58.41	0.98	0.17

Fan Voltage (V)	v @ 30 mm	v @ 40 mm	v @ 50 mm	v @ 60 mm	v @ 70 mm	Voltage (V)	Current (A)	Power (W)
12	21.81	22.28	22.65	22.28	22.28	29.28	0.34	9.96
12	21.81	22.28	22.65	22.28	22.28	29.28	0.34	9.96
12	21.81	22.28	22.65	22.28	22.28	29.28	0.34	9.96
12	21.81	22.28	22.65	22.28	22.28	29.28	0.34	9.96
12	21.81	22.28	22.65	22.28	22.28	29.28	0.34	9.96
12	21.81	22.28	22.65	22.28	22.28	29.28	0.34	9.96
12	21.81	22.28	22.65	22.28	22.28	29.28	0.34	9.96
12	21.81	22.28	22.65	22.28	22.28	29.28	0.34	9.96
12	21.81	22.28	22.65	22.28	22.28	29.28	0.34	9.96
12	21.81	22.28	22.65	22.28	22.28	29.28	0.34	9.96
12	21.81	22.28	22.65	22.28	22.28	29.28	0.34	9.96
12	21.81	22.28	22.65	22.28	22.28	29.28	0.34	9.96
12	21.81	22.28	22.65	22.28	22.28	29.28	0.34	9.96
12	21.81	22.28	22.65	22.28	22.28	29.28	0.34	9.96
12	21.81	22.28	22.65	22.28	22.28	29.28	0.34	9.96
12	21.81	22.28	22.65	22.28	22.28	29.28	0.34	9.96
12	21.81	22.28	22.65	22.28	22.28	29.28	0.34	9.96
12	21.81	22.28	22.65	22.28	22.28	29.28	0.34	9.96
12	21.81	22.28	22.65	22.28	22.28	29.28	0.34	9.96
12	21.81	22.28	22.65	22.28	22.28	29.28	0.34	9.96
12	21.81	22.28	22.65	22.28	22.28	29.28	0.34	9.96
12	21.81	22.28	22.65	22.28	22.28	29.28	0.34	9.96
12	21.81	22.28	22.65	22.28	22.28	29.28	0.34	9.96
12	21.81	22.28	22.65	22.28	22.28	29.28	0.34	9.96

12	21.81	22.28	22.65	22.28	22.28	29.28	0.34	9.96
12	21.81	22.28	22.65	22.28	22.28	29.28	0.34	9.96
12	21.81	22.28	22.65	22.28	22.28	29.28	0.34	9.96
12	21.81	22.28	22.65	22.28	22.28	29.28	0.34	9.96
12	21.81	22.28	22.65	22.28	22.28	29.28	0.34	9.96
12	21.81	22.28	22.65	22.28	22.28	29.28	0.34	9.96
12	21.81	22.28	22.65	22.28	22.28	29.28	0.34	9.96
12	21.81	22.28	22.65	22.28	22.28	29.28	0.34	9.96
12	21.81	22.28	22.65	22.28	22.28	29.28	0.34	9.96
12	21.81	22.28	22.65	22.28	22.28	29.28	0.34	9.96
12	21.81	22.28	22.65	22.28	22.28	29.28	0.34	9.96
12	21.81	22.28	22.65	22.28	22.28	29.28	0.34	9.96
12	21.81	22.28	22.65	22.28	22.28	29.28	0.34	9.96
12	21.81	22.28	22.65	22.28	22.28	29.28	0.34	9.96
12	21.81	22.28	22.65	22.28	22.28	29.28	0.34	9.96
12	21.81	22.28	22.65	22.28	22.28	29.28	0.34	9.96
12	21.81	22.28	22.65	22.28	22.28	29.28	0.34	9.96
12	21.81	22.28	22.65	22.28	22.28	29.28	0.34	9.96
12	21.81	22.28	22.65	22.28	22.28	29.28	0.34	9.96
12	21.81	22.28	22.65	22.28	22.28	29.28	0.34	9.96
12	21.81	22.28	22.65	22.28	22.28	29.28	0.34	9.96
12	21.81	22.28	22.65	22.28	22.28	29.28	0.34	9.96
12	21.81	22.28	22.65	22.28	22.28	29.28	0.34	9.96
12	21.81	22.28	22.65	22.28	22.28	29.28	0.34	9.96
12	21.81	22.28	22.65	22.28	22.28	29.28	0.34	9.96
12	21.81	22.28	22.65	22.28	22.28	29.28	0.34	9.96
12	21.81	22.28	22.65	22.28	22.28	29.28	0.34	9.96
12	21.81	22.28	22.65	22.28	22.28	29.28	0.34	9.96
12	21.81	22.28	22.65	22.28	22.28	29.28	0.34	9.96
12	21.81	22.28	22.65	22.28	22.28	29.28	0.34	9.96
12	21.81	22.28	22.65	22.28	22.28	29.28	0.34	9.96
12	21.81	22.28	22.65	22.28	22.28	29.28	0.34	9.96
12	21.81	22.28	22.65	22.28	22.28	29.28	0.34	9.96
12	21.81	22.28	22.65	22.28	22.28	29.28	0.34	9.96
12	21.81	22.28	22.65	22.28	22.28	29.28	0.34	9.96
12	21.81	22.28	22.65	22.28	22.28	29.28	0.34	9.96
12	21.81	22.28	22.65	22.28	22.28	29.28	0.34	9.96
12	21.81	22.28	22.65	22.28	22.28	29.28	0.34	9.96
12	21.81	22.28	22.65	22.28	22.28	29.28	0.34	9.96
12	21.81	22.28	22.65	22.28	22.28	29.28	0.34	9.96
12	21.81	22.28	22.65	22.28	22.28	29.28	0.34	9.96
12	21.81	22.28	22.65	22.28	22.28	29.28	0.34	9.96

12	21.81	22.28	22.65	22.28	22.28	29.28	0.34	9.96
12	21.81	22.28	22.65	22.28	22.28	29.28	0.34	9.96
12	21.81	22.28	22.65	22.28	22.28	29.28	0.34	9.96
12	21.81	22.28	22.65	22.28	22.28	29.28	0.34	9.96
12	21.81	22.28	22.65	22.28	22.28	29.28	0.34	9.96
12	21.81	22.28	22.65	22.28	22.28	29.28	0.34	9.96
12	21.81	22.28	22.65	22.28	22.28	29.28	0.34	9.96
12	21.81	22.28	22.65	22.28	22.28	29.28	0.34	9.96
12	21.81	22.28	22.65	22.28	22.28	29.28	0.34	9.96
12	21.81	22.28	22.65	22.28	22.28	29.28	0.34	9.96
12	21.81	22.28	22.65	22.28	22.28	29.28	0.34	9.96
12	21.81	22.28	22.65	22.28	22.28	29.28	0.34	9.96
12	21.81	22.28	22.65	22.28	22.28	29.28	0.34	9.96
12	21.81	22.28	22.65	22.28	22.28	29.28	0.34	9.96
12	21.81	22.28	22.65	22.28	22.28	29.28	0.34	9.96
12	21.81	22.28	22.65	22.28	22.28	29.28	0.34	9.96
12	21.81	22.28	22.65	22.28	22.28	29.28	0.34	9.96
12	21.81	22.28	22.65	22.28	22.28	29.28	0.34	9.96
12	21.81	22.28	22.65	22.28	22.28	29.28	0.34	9.96
12	21.81	22.28	22.65	22.28	22.28	29.28	0.34	9.96
12	21.81	22.28	22.65	22.28	22.28	29.28	0.34	9.96
12	21.81	22.28	22.65	22.28	22.28	29.28	0.34	9.96
12	21.81	22.28	22.65	22.28	22.28	29.28	0.34	9.96
12	21.81	22.28	22.65	22.28	22.28	29.28	0.34	9.96
12	21.81	22.28	22.65	22.28	22.28	29.28	0.34	9.96
12	21.81	22.28	22.65	22.28	22.28	29.28	0.34	9.96
12	21.81	22.28	22.65	22.28	22.28	29.28	0.34	9.96
12	21.81	22.28	22.65	22.28	22.28	29.28	0.34	9.96
12	21.81	22.28	22.65	22.28	22.28	29.28	0.34	9.96
12	21.81	22.28	22.65	22.28	22.28	29.28	0.34	9.96
12	21.81	22.28	22.65	22.28	22.28	29.28	0.34	9.96
12	21.81	22.28	22.65	22.28	22.28	29.28	0.34	9.96
12	21.81	22.28	22.65	22.28	22.28	29.28	0.34	9.96
12	21.81	22.28	22.65	22.28	22.28	29.28	0.34	9.96
12	21.81	22.28	22.65	22.28	22.28	29.28	0.34	9.96
12	21.81	22.28	22.65	22.28	22.28	29.28	0.34	9.96
12	21.81	22.28	22.65	22.28	22.28	29.28	0.34	9.96
12	21.81	22.28	22.65	22.28	22.28	29.28	0.34	9.96
12	21.81	22.28	22.65	22.28	22.28	29.28	0.34	9.96
12	21.81	22.28	22.65	22.28	22.28	29.28	0.34	9.96
12	21.81	22.28	22.65	22.28	22.28	29.28	0.34	9.96
12	21.81	22.28	22.65	22.28	22.28	29.28	0.34	9.96

12	21.81	22.28	22.65	22.28	22.28	29.28	0.34	9.96
12	21.81	22.28	22.65	22.28	22.28	29.28	0.34	9.96
12	21.81	22.28	22.65	22.28	22.28	29.28	0.34	9.96
12	21.81	22.28	22.65	22.28	22.28	29.28	0.34	9.96
12	21.81	22.28	22.65	22.28	22.28	29.28	0.34	9.96
12	21.81	22.28	22.65	22.28	22.28	29.28	0.34	9.96
12	21.81	22.28	22.65	22.28	22.28	29.28	0.34	9.96
12	21.81	22.28	22.65	22.28	22.28	29.28	0.34	9.96
12	21.81	22.28	22.65	22.28	22.28	29.28	0.34	9.96
12	21.81	22.28	22.65	22.28	22.28	29.28	0.34	9.96
12	21.81	22.28	22.65	22.28	22.28	29.28	0.34	9.96
12	21.81	22.28	22.65	22.28	22.28	29.28	0.34	9.96
12	21.81	22.28	22.65	22.28	22.28	29.28	0.34	9.96
12	21.81	22.28	22.65	22.28	22.28	29.28	0.34	9.96
12	21.81	22.28	22.65	22.28	22.28	29.28	0.34	9.96
12	21.81	22.28	22.65	22.28	22.28	29.28	0.34	9.96
12	21.81	22.28	22.65	22.28	22.28	29.28	0.34	9.96
12	21.81	22.28	22.65	22.28	22.28	29.28	0.34	9.96
12	21.81	22.28	22.65	22.28	22.28	29.28	0.34	9.96
12	21.81	22.28	22.65	22.28	22.28	29.28	0.34	9.96
12	21.81	22.28	22.65	22.28	22.28	29.28	0.34	9.96
12	21.81	22.28	22.65	22.28	22.28	29.28	0.34	9.96
12	21.81	22.28	22.65	22.28	22.28	29.28	0.34	9.96
12	21.81	22.28	22.65	22.28	22.28	29.28	0.34	9.96
12	21.81	22.28	22.65	22.28	22.28	29.28	0.34	9.96
12	21.81	22.28	22.65	22.28	22.28	29.28	0.34	9.96
12	21.81	22.28	22.65	22.28	22.28	29.28	0.34	9.96
12	21.81	22.28	22.65	22.28	22.28	29.28	0.34	9.96
12	21.81	22.28	22.65	22.28	22.28	29.28	0.34	9.96
12	21.81	22.28	22.65	22.28	22.28	29.28	0.34	9.96
12	21.81	22.28	22.65	22.28	22.28	29.28	0.34	9.96
12	21.81	22.28	22.65	22.28	22.28	29.28	0.34	9.96
12	21.81	22.28	22.65	22.28	22.28	29.28	0.34	9.96
12	21.81	22.28	22.65	22.28	22.28	29.28	0.34	9.96
12	21.81	22.28	22.65	22.28	22.28	29.28	0.34	9.96
12	21.81	22.28	22.65	22.28	22.28	29.28	0.34	9.96
12	21.81	22.28	22.65	22.28	22.28	29.28	0.34	9.96
12	21.81	22.28	22.65	22.28	22.28	29.28	0.34	9.96
12	21.81	22.28	22.65	22.28	22.28	29.28	0.34	9.96
12	21.81	22.28	22.65	22.28	22.28	29.28	0.34	9.96
12	21.81	22.28	22.65	22.28	22.28	29.28	0.34	9.96
12	21.81	22.28	22.65	22.28	22.28	29.28	0.34	9.96

12	21.81	22.28	22.65	22.28	22.28	29.28	0.34	9.96
12	21.81	22.28	22.65	22.28	22.28	29.28	0.34	9.96
12	21.81	22.28	22.65	22.28	22.28	29.28	0.34	9.96
12	21.81	22.28	22.65	22.28	22.28	29.28	0.34	9.96
12	21.81	22.28	22.65	22.28	22.28	29.28	0.34	9.96
12	21.81	22.28	22.65	22.28	22.28	29.28	0.34	9.96
12	21.81	22.28	22.65	22.28	22.28	29.28	0.34	9.96
12	21.81	22.28	22.65	22.28	22.28	29.28	0.34	9.96
12	21.81	22.28	22.65	22.28	22.28	29.28	0.34	9.96
12	21.81	22.28	22.65	22.28	22.28	29.28	0.34	9.96
12	21.81	22.28	22.65	22.28	22.28	29.28	0.34	9.96
12	21.81	22.28	22.65	22.28	22.28	29.28	0.34	9.96
12	21.81	22.28	22.65	22.28	22.28	29.28	0.34	9.96
12	21.81	22.28	22.65	22.28	22.28	29.28	0.34	9.96
12	21.81	22.28	22.65	22.28	22.28	29.28	0.34	9.96
12	21.81	22.28	22.65	22.28	22.28	29.28	0.34	9.96
12	21.81	22.28	22.65	22.28	22.28	29.28	0.34	9.96
12	21.81	22.28	22.65	22.28	22.28	29.28	0.34	9.96
12	21.81	22.28	22.65	22.28	22.28	29.28	0.34	9.96
12	21.81	22.28	22.65	22.28	22.28	29.28	0.34	9.96
12	21.81	22.28	22.65	22.28	22.28	29.28	0.34	9.96
								Avg.

h_1	Nu_1	Re	h_2	Nu_2
92.17	4.62	14970.51	88.09	4.41
92.11	4.61	14970.51	88.01	4.41
92.11	4.61	14970.51	88.03	4.41
92.12	4.62	14970.51	88.01	4.41
92.11	4.61	14970.51	88.01	4.41
92.12	4.62	14970.51	88.01	4.41
92.15	4.62	14970.51	88.02	4.41
92.18	4.62	14970.51	88.01	4.41
92.11	4.61	14970.51	87.95	4.41
92.04	4.61	14970.51	87.88	4.40
91.99	4.61	14970.51	87.84	4.40
92.03	4.61	14970.51	87.88	4.40
92.08	4.61	14970.51	87.93	4.41
92.04	4.61	14970.51	87.89	4.40
91.95	4.61	14970.51	87.79	4.40
92.01	4.61	14970.51	87.87	4.40
92.21	4.62	14970.51	88.03	4.41

92.19	4.62	14970.51	88.02	4.41
92.19	4.62	14970.51	88.00	4.41
92.17	4.62	14970.51	87.98	4.41
92.13	4.62	14970.51	87.95	4.41
92.09	4.61	14970.51	87.90	4.40
92.05	4.61	14970.51	87.87	4.40
92.00	4.61	14970.51	87.80	4.40
91.98	4.61	14970.51	87.77	4.40
92.06	4.61	14970.51	87.82	4.40
91.99	4.61	14970.51	87.80	4.40
91.95	4.61	14970.51	87.76	4.40
91.88	4.60	14970.51	87.71	4.39
91.82	4.60	14970.51	87.61	4.39
91.72	4.60	14970.51	87.54	4.39
91.72	4.60	14970.51	87.56	4.39
91.78	4.60	14970.51	87.61	4.39
91.77	4.60	14970.51	87.60	4.39
91.77	4.60	14970.51	87.57	4.39
91.88	4.60	14970.51	87.68	4.39
91.85	4.60	14970.51	87.66	4.39
91.85	4.60	14970.51	87.69	4.39
91.82	4.60	14970.51	87.63	4.39
91.80	4.60	14970.51	87.61	4.39
91.77	4.60	14970.51	87.58	4.39
91.75	4.60	14970.51	87.56	4.39
91.76	4.60	14970.51	87.58	4.39
91.80	4.60	14970.51	87.58	4.39
91.79	4.60	14970.51	87.55	4.39
91.81	4.60	14970.51	87.58	4.39
91.84	4.60	14970.51	87.63	4.39
91.78	4.60	14970.51	87.57	4.39
91.68	4.59	14970.51	87.47	4.38
91.76	4.60	14970.51	87.54	4.39
91.87	4.60	14970.51	87.62	4.39
91.81	4.60	14970.51	87.58	4.39
91.78	4.60	14970.51	87.57	4.39
91.85	4.60	14970.51	87.63	4.39
91.91	4.60	14970.51	87.66	4.39
91.86	4.60	14970.51	87.64	4.39
91.80	4.60	14970.51	87.59	4.39
91.80	4.60	14970.51	87.56	4.39
91.82	4.60	14970.51	87.56	4.39

91.77	4.60	14970.51	87.51	4.38
91.73	4.60	14970.51	87.47	4.38
91.69	4.59	14970.51	87.41	4.38
91.67	4.59	14970.51	87.38	4.38
91.56	4.59	14970.51	87.30	4.37
91.59	4.59	14970.51	87.31	4.37
91.56	4.59	14970.51	87.26	4.37
91.46	4.58	14970.51	87.17	4.37
91.47	4.58	14970.51	87.17	4.37
91.47	4.58	14970.51	87.15	4.37
91.46	4.58	14970.51	87.15	4.37
91.51	4.58	14970.51	87.19	4.37
91.59	4.59	14970.51	87.24	4.37
91.60	4.59	14970.51	87.27	4.37
91.65	4.59	14970.51	87.33	4.38
91.71	4.59	14970.51	87.40	4.38
91.64	4.59	14970.51	87.34	4.38
91.58	4.59	14970.51	87.29	4.37
91.62	4.59	14970.51	87.34	4.38
91.64	4.59	14970.51	87.32	4.37
91.63	4.59	14970.51	87.31	4.37
91.58	4.59	14970.51	87.24	4.37
91.52	4.59	14970.51	87.18	4.37
91.51	4.58	14970.51	87.19	4.37
91.51	4.58	14970.51	87.20	4.37
91.54	4.59	14970.51	87.21	4.37
91.51	4.58	14970.51	87.21	4.37
91.49	4.58	14970.51	87.17	4.37
91.45	4.58	14970.51	87.15	4.37
91.50	4.58	14970.51	87.17	4.37
91.50	4.58	14970.51	87.17	4.37
91.45	4.58	14970.51	87.13	4.37
91.48	4.58	14970.51	87.16	4.37
91.47	4.58	14970.51	87.12	4.36
91.44	4.58	14970.51	87.11	4.36
91.40	4.58	14970.51	87.07	4.36
91.30	4.57	14970.51	86.97	4.36
91.30	4.57	14970.51	86.98	4.36
91.36	4.58	14970.51	87.03	4.36
91.42	4.58	14970.51	87.10	4.36
91.44	4.58	14970.51	87.12	4.36
91.48	4.58	14970.51	87.16	4.37

91.47	4.58	14970.51	87.16	4.37
91.42	4.58	14970.51	87.12	4.36
91.45	4.58	14970.51	87.11	4.36
91.48	4.58	14970.51	87.13	4.37
91.48	4.58	14970.51	87.13	4.37
91.45	4.58	14970.51	87.13	4.37
91.47	4.58	14970.51	87.17	4.37
91.52	4.58	14970.51	87.18	4.37
91.51	4.58	14970.51	87.17	4.37
91.50	4.58	14970.51	87.15	4.37
91.49	4.58	14970.51	87.15	4.37
91.48	4.58	14970.51	87.14	4.37
91.51	4.58	14970.51	87.18	4.37
91.53	4.59	14970.51	87.18	4.37
91.42	4.58	14970.51	87.07	4.36
91.38	4.58	14970.51	87.04	4.36
91.44	4.58	14970.51	87.10	4.36
91.47	4.58	14970.51	87.10	4.36
91.50	4.58	14970.51	87.10	4.36
91.47	4.58	14970.51	87.09	4.36
91.41	4.58	14970.51	87.05	4.36
91.35	4.58	14970.51	86.98	4.36
91.34	4.58	14970.51	86.97	4.36
91.29	4.57	14970.51	86.91	4.35
91.23	4.57	14970.51	86.86	4.35
91.22	4.57	14970.51	86.84	4.35
91.23	4.57	14970.51	86.85	4.35
91.20	4.57	14970.51	86.83	4.35
91.15	4.57	14970.51	86.79	4.35
91.19	4.57	14970.51	86.81	4.35
91.27	4.57	14970.51	86.88	4.35
91.30	4.57	14970.51	86.94	4.36
91.27	4.57	14970.51	86.91	4.35
91.23	4.57	14970.51	86.85	4.35
91.22	4.57	14970.51	86.84	4.35
91.21	4.57	14970.51	86.81	4.35
91.16	4.57	14970.51	86.80	4.35
91.15	4.57	14970.51	86.77	4.35
91.14	4.57	14970.51	86.77	4.35
91.14	4.57	14970.51	86.75	4.35
91.15	4.57	14970.51	86.74	4.35
91.21	4.57	14970.51	86.79	4.35

91.22	4.57	14970.51	86.80	4.35
91.18	4.57	14970.51	86.78	4.35
91.14	4.57	14970.51	86.73	4.35
91.06	4.56	14970.51	86.65	4.34
91.00	4.56	14970.51	86.61	4.34
91.13	4.57	14970.51	86.72	4.34
91.16	4.57	14970.51	86.76	4.35
91.09	4.56	14970.51	86.71	4.34
91.03	4.56	14970.51	86.65	4.34
90.96	4.56	14970.51	86.58	4.34
91.08	4.56	14970.51	86.71	4.34
91.12	4.57	14970.51	86.74	4.35
91.07	4.56	14970.51	86.69	4.34
91.01	4.56	14970.51	86.63	4.34
91.02	4.56	14970.51	86.66	4.34
91.02	4.56	14970.51	86.68	4.34
91.05	4.56	14970.51	86.68	4.34
91.05	4.56	14970.51	86.71	4.34
91.01	4.56	14970.51	86.65	4.34
90.93	4.56	14970.51	86.57	4.34
90.98	4.56	14970.51	86.61	4.34
91.06	4.56	14970.51	86.68	4.34
91.11	4.56	14970.51	86.74	4.35
91.09	4.56	14970.51	86.72	4.34
91.08	4.56	14970.51	86.72	4.34
91.08	4.56	14970.51	86.69	4.34
91.07	4.56	14970.51	86.68	4.34
91.00	4.56	14970.51	86.63	4.34
91.55	4.59	14970.51	87.26	4.37